

Matti Pajari

Resistance of prestressed hollow core slabs against web shear failure

Resistance of prestressed hollow core slabs against web shear failure

Matti Pajari

VTT Building and Transport



ISBN 951-38-6709-9 (soft back ed.)
ISSN 1235-0605 (soft back ed.)

ISBN 951-38-6552-5 (URL: <http://www.vtt.fi/inf/pdf/>)
ISSN 1455-0865 (URL: <http://www.vtt.fi/inf/pdf/>)

Copyright © VTT 2005

JULKAISIJA – UTGIVARE – PUBLISHER

VTT, Vuorimiehentie 5, PL 2000, 02044 VTT
puh. vaihde 020 722 111, faksi 020 722 4374

VTT, Bergsmansvägen 5, PB 2000, 02044 VTT
tel. växel 020 722 111, fax 020 722 4374

VTT Technical Research Centre of Finland, Vuorimiehentie 5, P.O.Box 2000, FI-02044 VTT, Finland
phone internat. +358 20 722 111, fax +358 20 722 4374

VTT Rakennus- ja yhdyskuntatekniikka, Kemistintie 3, PL 1805, 02044 VTT
puh. vaihde 020 722 111, faksi 020 722 7007

VTT Bygg och transport, Kemistvägen 3, PB 1805, 02044 VTT
tel. växel 020 722 111, fax 020 722 7007

VTT Building and Transport, Kemistintie 3, P.O.Box 1805, FI-02044 VTT, Finland
phone internat. +358 20 722 111, fax +358 20 722 7007

Technical editing Leena Ukaskoski

Otamedia Oy, Espoo 2005

Pajari, Matti. Resistance of prestressed hollow core slabs against web shear failure. Espoo 2005. VTT Tiedotteita – Research Notes 2292. 47 p. + app. 15 p.

Keywords hollow core slab, prestress, shear, test, resistance, concrete, precast, structure, design, Eurocode

Abstract

Eurocode 2 presents a design method for the shear resistance, which according to harmonized standard EN 1168 is to be used for the web shear failure of prestressed hollow core slabs. To check the validity of the method, 49 shear tests on hollow core slabs with thickness 200–500 mm have been analysed.

The Eurocode 2 method overestimated the mean shear resistance of all tested slab types. For 200 mm slabs and slabs with flat webs the overestimation was tens of percent. When the characteristic values of experimental and theoretical resistance were compared, the fit was better but there was still a considerable overestimation for 200 mm slabs and for the slabs with flat webs. On the other hand, the Eurocode 2 method was (over)conservative for 265 mm and 320 mm slabs with circular voids.

The Eurocode 2 method ignores the shear stresses due to the transfer of the prestressing force. When these stresses were taken into account applying Yang's method, the accuracy for 265 mm and 320 mm slabs with circular voids was the same as when using the Eurocode 2 method but much better for the other slabs.

Based on the results of the comparison, Yang's method for design against web shear failure should replace the present method in Eurocode 2. It is not acceptable, however, to adopt a design method which overestimates the characteristic resistance of some product type by 10% as Yang's method seems to do. Whether this is really the case, is still an open question because the number of tests on the problematic slabs was small. Furthermore, due to the nature of the type approval tests, some test specimens may have been weaker than the slabs typical of normal production.

The Eurocode 2 method should not be used for slabs with flat webs without a reduction factor, and its applicability to other slab types should always be verified either numerically or experimentally before it is used.

Preface

In the future, prestressed hollow core slabs will be provided with a CE-marking. This means that the producer has to determine and declare the essential properties of the slabs in accordance with standard EN 1168. As regards the mechanical resistance, EN 1168 refers to the European standard EN 1992 called Eurocode 2.

Since the early seventies, roughly one thousand load tests on single prestressed hollow core slabs have been performed at VTT. In these tests it has been observed that the calculation method for shear resistance given in Eurocode 2 seems to work well for slabs with circular voids, but when applied to slabs with noncircular voids and flat webs, it gives nonconservative results. To quantify this effect and to facilitate the future development of EN 1168, theoretical and experimental results have been compared. All relevant tests carried out by VTT since 1990 have been considered.

The project has been financed by the Confederation of Finnish Construction Industries RT and VTT and coordinated by Arto Suikka from RT. Special thanks are due to the following companies which have permitted the use and publication of their confidential test results:

Ansion Sementtivalimo Oy

Consolis Oy

Betsset Oy

Lakan Betoni oy

Lujabetoni Oy

Parma Oy

Pielisen Betoni Oy

Rautaruukki Oy

Teräspeikko Oy.

Contents

Abstract.....	3
Preface	4
List of symbols	6
1. Introduction.....	9
2. Design against web shear failure	13
2.1 Failure criterion	13
2.2 Shear resistance, traditional approach	14
2.3 Shear resistance, Yang’s method.....	15
3. Tests	18
4. Analysis of test results	25
4.1 Assumptions	25
4.1.1 Material behaviour	25
4.1.2 Geometry.....	27
4.2 Comparison of predicted and observed resistance	28
4.2.1 Predicted resistance calculated using mean tensile strength.....	28
4.2.2 Predicted resistance calculated using characteristic tensile strength ...	31
4.2.3 Location of critical point.....	39
5. Discussion.....	42
5.1 Assesment of tests	42
5.2 Results from other researchers	43
5.3 Mean or characteristic resistance?.....	44
5.4 Comparison of EC2 vs. Yang’s method.....	44
6. Summary and conclusions	45
References	47
Appendices	
Appendix A: Expression for shear stress	
Appendix B: Criterion for bond slip	
Appendix C: Data about tests	

List of symbols

A	cross-sectional area of slab
A_{cp}	cross-sectional area of slab above considered point (or axis)
E_c	elasticity modulus of concrete
$E_{C,28}$	elasticity modulus of concrete at age of 28 days
E_p	elasticity modulus of prestressing steel
F	concentrated load
H	thickness of slab
I	second moment of area of cross-section
I_w	second moment of area when flanges outside web width are excluded
L	span length
M	Bending moment due to self-weight and imposed load
P	effective prestressing force
P_i	effective prestressing force in tendon layer i
S	first moment of area
S_{cp}	first moment of area of section above considered point
S_w	first moment of area, flanges outside web width excluded
V	shear force
V_c	resistance against web shear failure (shear resistance)
V_g	shear force at support due to self-weight of slab
V_{obs}	observed shear resistance = shear force at support at failure

V_{pre}	predicted shear resistance = shear force at support at failure
a	shear span = distance from support to the nearest line load
b_w	sum of web widths $b_{w,i}$
$b_{w,i}$	width of web i (width of neck between adjacent voids or between void and slab edge)
b_1, \dots, b_4	geometric parameters for nominal slab cross-section
e (e_i)	eccentricity of tendon (tendon layer i), positive downwards from centroidal axis
f_{ck}	$= f_{ck,C150}$, characteristic strength of concrete, 150 x 300 mm cylinder strength
$f_{ck,C50}$	characteristic strength of concrete, 50 mm cylinder strength
$f_{ck,K150}$	characteristic strength of concrete, 150 mm cube strength
f_{ct}	tensile strength of concrete
f_{ctd}	design value of tensile strength of concrete $= f_{ctk} / \gamma_c$
f_{ctm}	mean tensile strength of concrete
f_{ctk}	characteristic tensile strength of concrete
h	vertical distance to soffit
h_{cp}	vertical distance to soffit from the considered point
h_1, \dots, h_4	geometric parameters for nominal slab cross-section
l_{pt}	basic value of transfer length
r_1, \dots, r_2	geometric parameters for nominal slab cross-section
t_b	width of bearing
t_{rel}	age of concrete at release of prestressing force

x	axial coordinate, origin at support
z	vertical coordinate, origin at centroidal axis, positive downwards
z_{cp}	vertical coordinate of considered point
α_1	bond parameter
α_2	bond parameter
χ_i	ratio of observed to predicted resistance in test i
χ_{mean}	mean of χ_i -values
χ_{stdev}	standard deviation of χ_i -values
$\chi_{5\%}$	5% quantile of χ_i -values
γ_c	safety factor of concrete
η_{p1}	bond parameter
η_i	bond parameter
ϕ	diameter of strand
σ	axial normal stress
σ_I	maximum principal stress
σ_{cp}	concrete stress at considered point
σ_{p0}	initial prestress in tendon
τ	shear stress
τ_{cp}	shear stress at considered point

1. Introduction

In Finland, the first prestressed hollow core slabs were 150, 200 or 265 mm in thickness. They were provided with circular voids. Since the early eighties, slab cross-sections with non-circular voids became gradually popular, first in 400 mm thick slabs, then in 320, 370 and 500 mm thick slabs. The typical cross-sections of such slabs look like the ones shown in Figure 1. The inner webs have a constant thickness over a depth of $H/3-H/2$. The outermost webs are only slightly tapered due to the non-verticality of the outer edges.

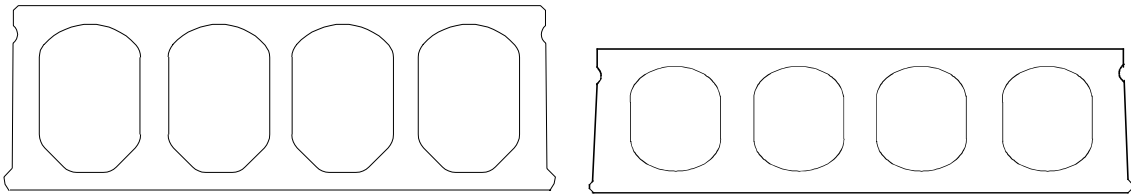


Figure 1. Typical slab cross-sections with non-circular voids used in Finland.

It was soon realized that the resistance of the new slabs against web shear failure was considerably lower than that predicted by the traditional design method presented e.g. in FIP Recommendations [7]. The traditional method, on the other hand, resulted in a good fit with the test results when applied to slabs with circular voids. To allow for this difference, a reduction factor to the FIP formula was proposed [8].

The expression for shear resistance given in FIP Recommendations is based on the work done by Walraven & Mercx [9]. They also noticed that the observed shear resistance was lower than the predicted one when the voids were noncircular. They explained the effect by the probability theory. In slabs with circular voids the failure in the web may only take place at the depth where the web is narrowest. In slabs similar to those in Figure 1, the tensile stress due to the shear force is nearly constant over a major area in vertical direction which makes the local weaknesses more likely to occur in the highly stressed zone, and in this way may make the slab fail at a lower load.

It has also been proposed that the tensile strength of the concrete is not the same in all parts of the slab cross-section and the tensile strength also varies from one section to another. So, the tensile strength determined from cores drilled from the top flange may not reflect the true tensile strength in the web.

One explanation to the lower-than-expected shear resistance is the inaccuracy of the traditional design rules in prediction of the maximum tensile stress in the webs for sections like those shown in Figure 1. This is discussed in the rest of this chapter.

For heavily prestressed hollow core slabs subjected to a high shear force and a moderate bending moment, a shear failure in the web close to the support is often observed in load tests. Figure 2 illustrates a model for analysis of such a case. One longitudinal slice of an extruded 265 mm slab is taken into consideration. It is replaced by another slice having the cross-section shown in Figure 2.b, the width of which varies stepwise in vertical direction. The latter slice is modelled by two dimensional, quadratic, isoparametric solid elements, the thickness of which varies accordingly. The element mesh is shown in Figure 2.c. A vertical point load, corresponding to a typical experimental failure load, is placed on the top of the model at a distance of 1000 mm from the support. There are two 93 mm² strands per web, each with prestress 1000 MPa. The prestressing force is transferred in the model as shown in Figure 3. Assuming linear material behaviour, the distribution of principal stresses shown in Figure 4 is obtained.

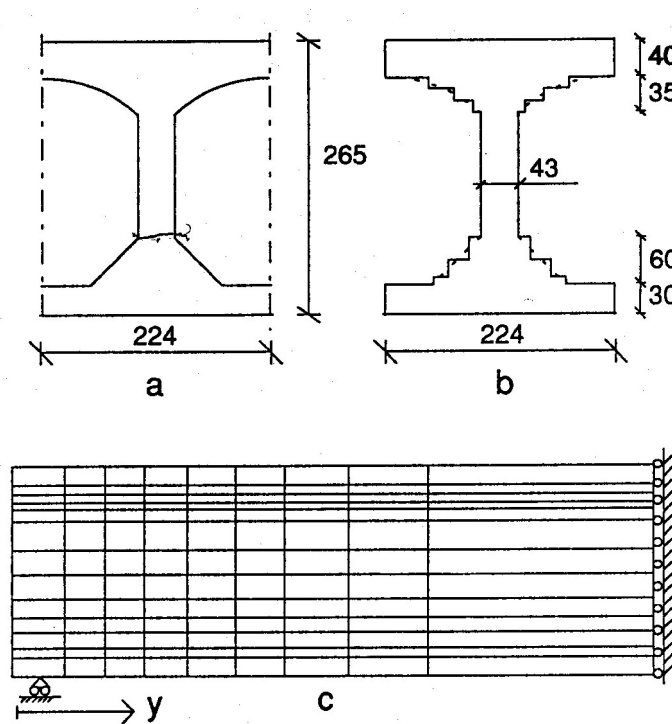


Figure 2. a) Cross-section of one web and the flanges on both sides. b) Approximate cross-section for two dimensional FEM-model. c) Side view on FEM-model. There is a vertical point load at the right end of the model corresponding to 200 kN / 1,2 m.

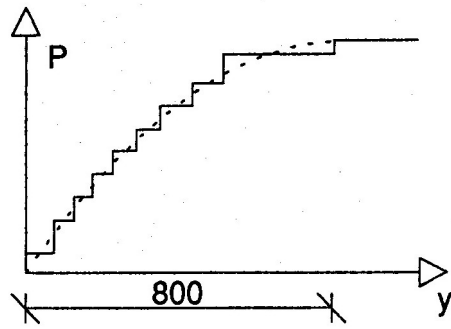


Figure 3. Assumed transfer of prestressing force (dashed line) and as modelled (continuous stepwise line).

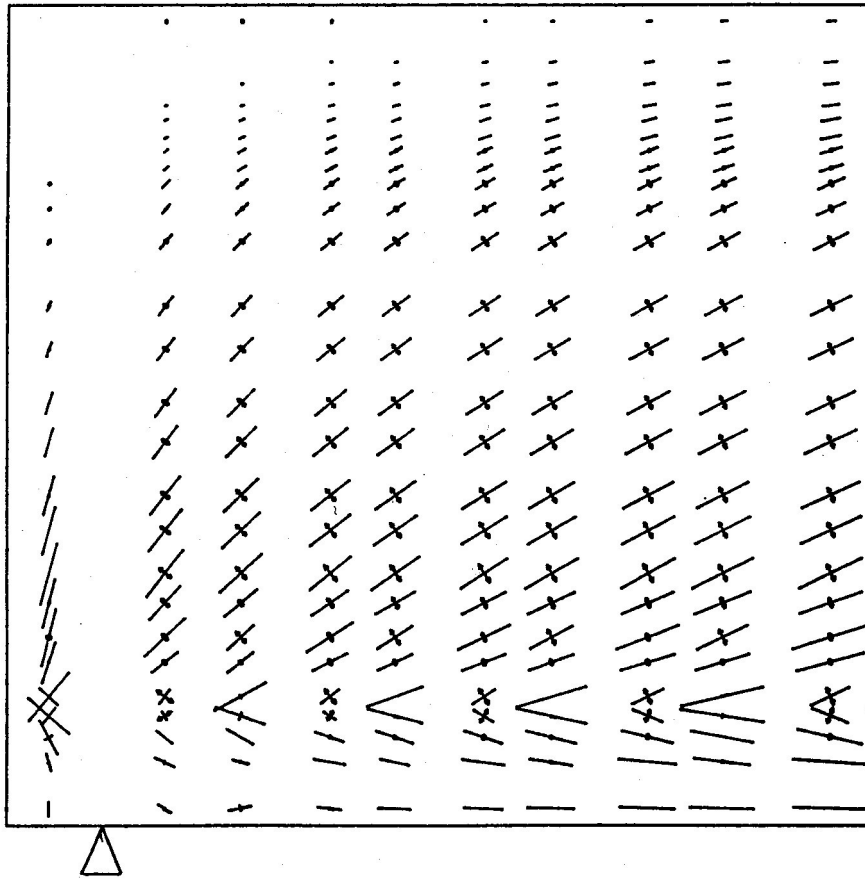


Figure 4. Principal stresses illustrated as vectors. Tensile stresses are indicated by arrows.

There are tensile stresses in the web outside the support zone, the maximum tensile stress being of the order of the mean tensile strength. The maximum tensile stress is not located at the centroidal axis as it should according to Eurocode 2 (EC2) [5], Eq. 6.4. In

addition, the magnitude of the maximum principal stress is underestimated by EC2. The FE analysis takes into account the shear stresses due to the prestressing force ignored by EC2. This is the main reason for the different results given by these two procedures. Since the FE-analysis yields results which are at least qualitatively in accordance with experimental data, it is tempting to analyse several test results with the FEM. This has been done by Yang [10].

Yang [10] has also proposed a simple design method which takes the shear stresses due to the transfer of the prestressing force into account. Yang's method, in which the shear stresses are derived from Navier's bending theory, gave good correspondence with test results, when the material parameters were evaluated from the test results in accordance with the Swedish concrete code [1].

In the future, the prestressed hollow core slabs have to be provided with a CE marking. This means that the slabs have to be designed according to the standard EN 1168 [4], which means that they in the nearest future *can*, and in the long run, *will* be designed according to EC2. The aim of the present study is to check, how well the present design rule, i.e. Eq. 6.4 in EC2, predicts the experimental shear resistance. For comparison, the same check is also carried out using Yang's method.

2. Design against web shear failure

2.1 Failure criterion

Due to the short development length and lacking shear reinforcement in prestressed hollow core slabs, a diagonal shear crack in the web close to the support necessitates a failure. In such a case the failure criterion is formulated as

$$\sigma_I = f_{ct} \quad (1)$$

where f_{ct} is the uniaxial tensile strength of the concrete and σ_I denotes the maximum principal stress in the web obtained from

$$\sigma_I = \frac{\sigma}{2} + \sqrt{\left(\frac{\sigma}{2}\right)^2 + \tau^2} \quad (2)$$

where σ and τ are the horizontal normal stress and shear stress. The vertical normal stress due to the support pressure is taken into account in such a way, that the failure criterion is not applied too close to the support where the vertical stress component is effective and reduces σ_I .

It is well-known that not only the maximum principal stress but also the other principal stresses have to be taken into account in a general failure criterion. However, in the web of a prestressed hollow core slab, the stress state is essentially two-dimensional. Moreover, the compressive principal stress in the web is so small, that its effect on the transverse tensile strength is small. In this special case Eq. 1 can be regarded as a good approximation for failure criterion.

There has been a lot of discussion about the effective tensile strength and how it could be measured. Should it be measured directly from punching tests, splitting tests, dog bone tests or something else? Does the strength of the cores, drilled vertically from the top flange, reflect the strength of the concrete in the web? If so, how can the core strength be transformed into 150 x 300 mm cylinder strength and then into tensile strength, or should the tensile strength be determined directly from the cores?

There has been less discussion about the calculation of the maximum principal stress. This is strange because we have all reasons to believe that linear, two-dimensional elastic FEM analyses suit well for calibration of simple design rules provided that the transfer of the prestressing force from the tendons to the concrete is known.

2.2 Shear resistance, traditional approach

E.g. the British Code of Practice CP110 [3] has approximated that the shear resistance of the web is

$$V_c = \frac{b_w I_w}{S_w} \sqrt{f_{ct}^2 - 0,8 \sigma_{cp} f_{ct}} \quad (3)$$

where S_w and I_w are the first and second moment of area of the web, b_w is the web width, f_{ct} the tensile strength of the concrete and σ_{cp} the normal stress of the concrete at the centroidal axis, calculated from

$$\sigma_{cp} = \frac{-P}{A} \quad (4)$$

where P is the prestressing force acting at the considered cross-section and A the area of the concrete section. Walraven and Mercx [9] have proposed a similar formula

$$V_c = 0,75 \frac{b_w I}{S} \sqrt{f_{ct}^2 - \sigma_{cp} f_{ct}} \quad (5)$$

with a calibration factor of 0,75. I and S are calculated for the whole cross-section. σ_{cp} is calculated from Eq. 9 taking the prestressing force at the inner edge of the support. Eq. 5 is included in FIP Recommendations [7] without the calibration factor 0,75. EC2 has adopted Eq. 5 in the form of

$$V_c = \frac{b_w I}{S} \sqrt{f_{ct}^2 - \sigma_{cp} f_{ct}} \quad (6)$$

with the exception that σ_{cp} is calculated from Eq. 4 but P is the prestressing force at the considered section which is at a distance of $H/2$ from the inner edge of the support (H is the slab thickness). Eq. 6 is equivalent to Eqs 1 and 2 when the shear stress τ_{cp} is calculated from

$$\tau_{cp} = \frac{1}{b_w} \frac{S_{cp}}{I} V \quad (7)$$

According to Eq. 7, the maximum shear stress and hence, the maximum principal stress is obtained when S_{cp}/b_w has its maximum value. For hollow core sections with circular or oval voids, the maximum principal stress is obtained at the centroidal axis of the cross-section or close to it.

2.3 Shear resistance, Yang's method

Eq. 6 does not take into account the shear stresses due to the transfer of prestressing force. The existence of such shear stresses is evident from Figure 5. The lower part of the slab tends to contract when the prestressing force is released. Since the lower and upper part are coupled, there must be shear stresses that keep the parts together.

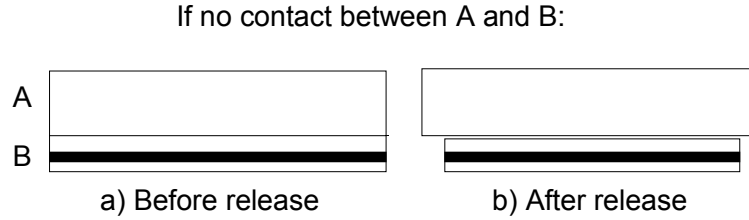


Figure 5. Illustration of what happens without shear stresses at the release of the prestressing force.

In the case of one tendon layer, Yang [10] has proposed that the shear stress be calculated from

$$\tau = \frac{1}{b_w} \left[\left(\frac{A_{cp}}{A} - \frac{S_{cp}e}{I} \right) \frac{dP}{dx} + \frac{S_{cp}}{I} V \right] \quad (8)$$

Here dP/dx is the gradient of the tendon forces, e is the eccentricity of tendon force and A_{cp} and S_{cp} the cross-sectional area and first moment of area above the considered axis, respectively. The first term

$$\tau_t = \frac{1}{b_w} \left(\frac{A_{cp}}{A} - \frac{S_{cp}e}{I} \right) \frac{dP}{dx} \quad (9)$$

is attributable to the transfer of the prestressing force. If it vanishes, Eq. 7 is obtained. In case of more than one tendon layer the normal stress is calculated from

$$\sigma = \frac{-\sum_i P_i}{A} + \frac{-\sum_i P_i e_i + M}{I} z \quad (10)$$

and the shear stress from

$$\tau = -\frac{1}{b} \left[\frac{A_{cp}}{A} \sum_i \frac{dP_i}{dx} - \frac{S_{cp}}{I} \sum_i e_i \frac{dP_i}{dx} + \frac{S_{cp}}{I} V - \sum_j \frac{dP_j}{dx} \right] \quad (11)$$

where P_i and e_i (negative above centroidal axis) are the force in and eccentricity of tendon layer i . M is the bending moment due to external loads at the considered section.

$\sum_j \frac{dP_j}{dx}$ represents the sum of all tendon force gradients above the considered axis. If

there is only one tendon layer at the bottom, Eq. 11 reduces to Eq. 8. Eq. 11 is derived in Appendix A.

Eqs 9 and 10 imply, that the maximum shear stress does not necessarily exist near to the centroidal axis. The maximum principal stress may be elsewhere, and hence the horizontal normal stress has to be calculated from Eq. 10 or in the case of one tendon layer from

$$\sigma = \frac{-P}{A} + \frac{-Pe + M}{I} z \quad (12)$$

According to Yang, the vertical compressive stress due to the support reaction is taken into account as shown in Figure 6. The critical point is located somewhere on a straight line A'B' shown in Figure 6.b. By choosing closely spaced points, hereafter called considered points, along the line and calculating the maximum principal stress in each of them, the critical point where the principal stress has its maximum value can be determined for each load case. By varying the load, the resistance against the web shear failure is determined.

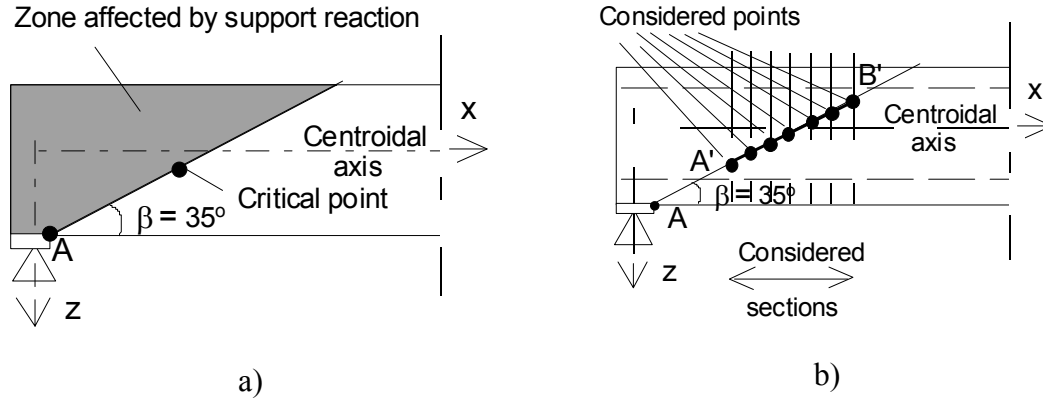


Figure 6. a) Possible location of critical point next to the zone affected by support reaction. b) Points and sections taken into consideration in calculations.

The geometric symbols are illustrated in Figure 7. The web width depends on z_{cp} and is obtained from

$$b_w = \sum_i b_{wi}(z_{cp}) \quad (13)$$

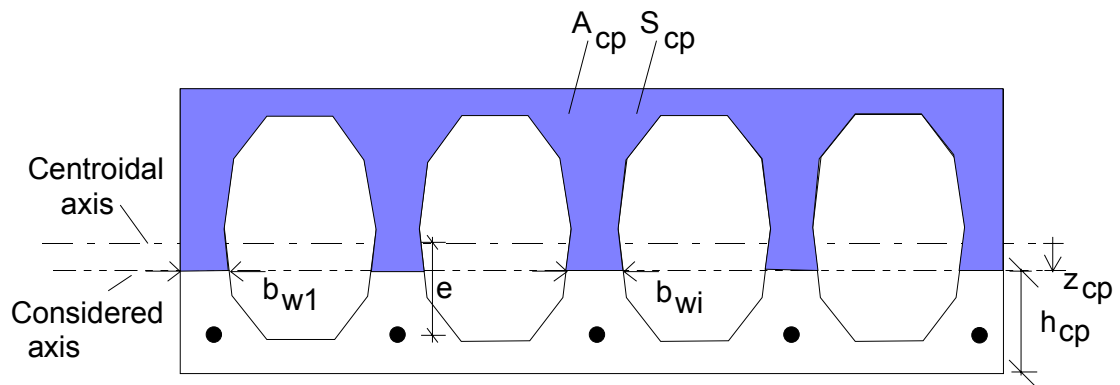


Figure 7. Illustration of geometric parameters of considered cross-section.

3. Tests

Since 1990, VTT has carried out hundreds of load tests on extruded prestressed hollow core slabs. The purpose of these tests has varied. There have been type approval tests, quality control tests (the majority), tests carried out in research projects or for product development, verification tests on slabs taken from site etc. All such tests have now been examined¹ and those which ended with shear tension failure in the web and were

- simply supported
- isolated (not a part of a floor)
- loaded with transverse, uniformly distributed line loads

were taken into closer consideration. From these were excluded only those in which

- the slabs had grouting at the loaded end
- some important data as the measured strength were missing
- the shear span (distance from support to the nearest line load) was less than 2,4 times the slab thickness
- the slippage of strands was greater than that acceptable in the Finnish quality control for type approved slabs, see Appendix B.

In this way, 49 slabs remained. All slab producers permitted the use and publication of their test results. Hence no slab was excluded due to the confidentiality. The number of accepted and excluded slabs are given in Table 1.

Table 1. Number of acceptable and excluded tests.

Thickness mm	Accepted tests	Rejected tests	Note
200	4	5	5 with circular, 5 with non-circular voids
265	20	7	
320	10	4	
370	2	3	
400	7	2	
500	6	2	
Total	49	23 (32%)	

¹ The tests carried out before 1990 have been reported in [8]. They are not considered here, because their documentation has been less accurate and because most of the slab cross-sections with non-circular voids tested in the eighties have been replaced by new types.

Figure 8 illustrates the geometric characteristics measured before each test. These include the length of the slab, the total width of the section at the bottom, at mid-depth and on the top, the depth of the section in the middle and at both edges, slippage for each strand, width and height of each hollow core, minimum thickness of the top flange, bottom flange and each web. In addition, the mass of each slab was measured.

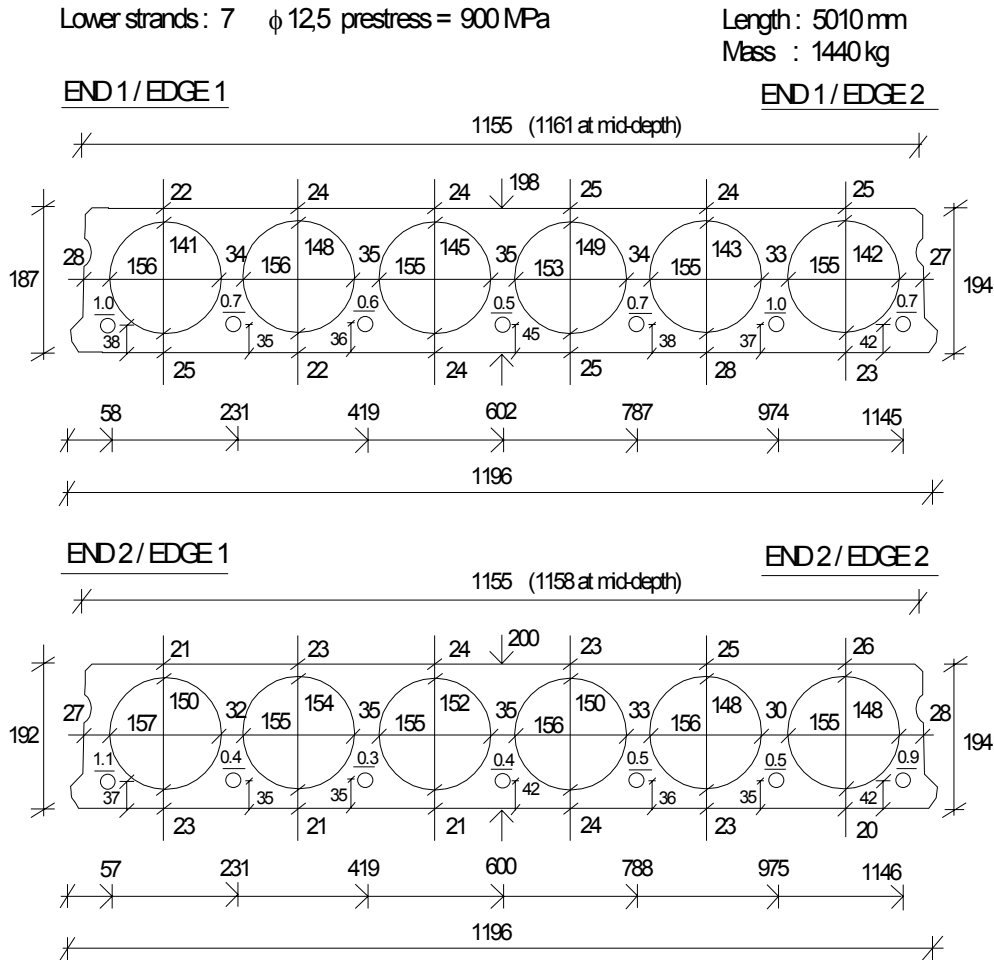


Figure 8. Cross-sectional characteristics measured for each slab unit.

After the load test, six 50 mm cores were drilled from each slab, or from one representative slab in case there were several identical slabs taken from the same casting bed and casting lot. The cores were tested immediately when still wet, or when this was not possible, the cores were kept in a closed plastic bag until testing.

The perimeter of the slabs was almost identical for all slab cross-sections with the same depth. On the contrary, the number, shape and size of the voids varied. In addition to the nominal width, the nominal geometry of the slab cross-sections can accurately enough be specified by the data given in Tables 2–4. Altogether, 15 different nominal geometries for concrete cross-section were identified in the accepted test specimens.

Table 2. Types, parameters, depths and core codes for tested slab cross-sections of type 1–3.

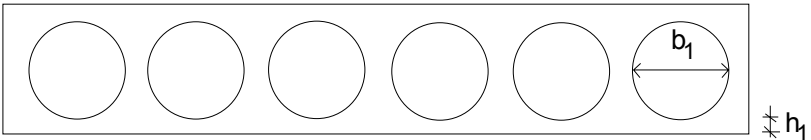
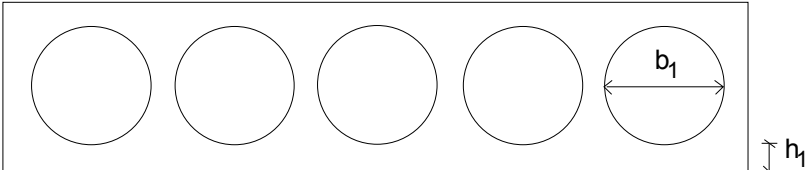
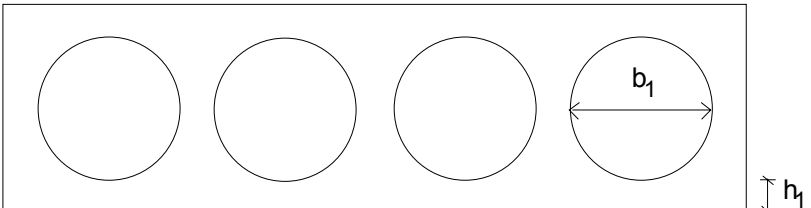
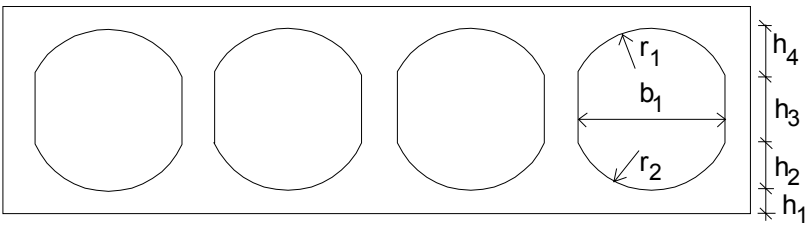
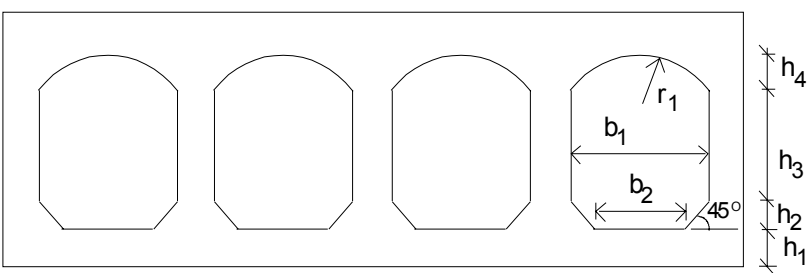
Type	Parameters	Depth mm	Core code
1		200	601 602
1		265	501 502 503
1		320	401
2		320 370 400	410 411 412 413 414 415
3		400	416

Table 3. Types, parameters, depths and core codes for tested slab cross-sections of type 4 and 5.

Type	Parameters	Depth mm	Core code
4		320	421
5		500	422

Table 4. Nominal values in millimetres for parameters shown in Table 3.

Code	H	b_1	b_2	b_3	b_4	r_1	r_2	h_1	h_2	h_3	h_4	h_5	h_6	h_7	h_8
601	200	150	0	0	0	0	0	25	0	0	0	0	0	0	0
602	200	155	0	0	0	0	0	25	0	0	0	0	0	0	0
501	265	185	0	0	0	0	0	40	0	0	0	0	0	0	0
502	265	191	0	0	0	0	0	39,5	0	0	0	0	0	0	0
503	320	185	0	0	0	0	0	67,5	0	0	0	0	0	0	0
401	320	229	0	0	0	0	0	40,5	0	0	0	0	0	0	0
410	320	220	0	0	0	122	122	38	69,24	105,52	69,24	0	0	0	0
411	320	222	0	0	0	123	123	36	70	106	70	0	0	0	0
412	370	220	0	0	0	122	122	63	69,24	105,52	69,24	0	0	0	0
413	400	225	0	0	0	112,5	112,5	40	112,5	95	112,5	0	0	0	0
414	400	223	0	0	0	111,5	111,5	35	111,5	102	111,5	0	0	0	0
415	400	222	0	0	0	123	123	36	70	186	70	0	0	0	0
416	400	221	97	0	0	125	0	40	62	191,44	66,56	0	0	0	0
421	320	229	0	41	0	126	126	35	73,41	103,2	73,41	84	71	21,57	0
422	500	215	70	40	86	120	0	48	72,5	248	66,67	50,5	250,36	80	6,86

In Table 5 the different load types are shown.

Table 5. Load types.

Type	Loading
1	<p>Diagram 1: A simply supported beam of length L with two pairs of point loads. The first pair is located at a distance of $L/7,2$ from the left support, and the second pair is located at a distance of $L/7,2$ from the right support. Each load is labeled $F/2$.</p>
2	<p>Diagram 2: A simply supported beam of length L with four point loads. From left to right, the loads are at distances $L/8$, $L/4$, $L/4$, and $L/8$ from the left support. Each load is labeled $F/2$.</p>
3	<p>Diagram 3: A simply supported beam of length L with two pairs of point loads. The first pair is at a distance a from the left support, and the second pair is at a distance a from the right support. Each load is labeled $F/2$. A dimension of 300 is shown between the two loads in each pair.</p>
4	<p>Diagram 4: A simply supported beam of length L with a single point load F at a distance a from the left support.</p>
5	<p>Diagram 5: A simply supported beam of length L with two point loads. The first load is at a distance a from the left support, and the second load is at a distance a from the right support. Each load is labeled $F/2$. A dimension of 300 is shown between the two loads.</p>
6	<p>Diagram 6: A simply supported beam of length L with a single point load F at a distance a from the left support.</p>

The weight of the cantilevered end in load type 6 as well as the weight of cast-in-situ concrete at the unloaded end of the test specimen in some tests are taken into account in the shear force due to the self-weight given in Appendix C, Table 4.

Figures 9–12 illustrate the loading arrangements. The soffit of a slab may be non-planar, which may result in a torque and reduced shear resistance when the slab is loaded. Measures to eliminate the torque are clarified in Figure 11.

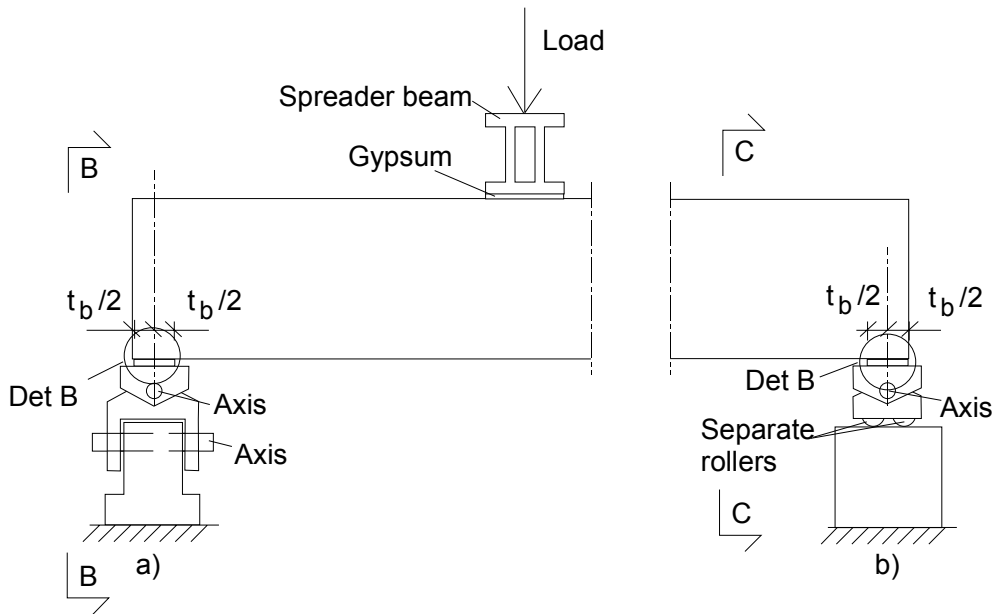


Figure 9. Side view on loading arrangements. For Det B see Figure 10.

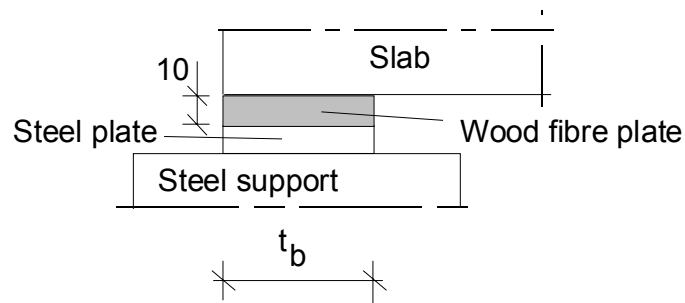


Figure 10. Arrangement at support.

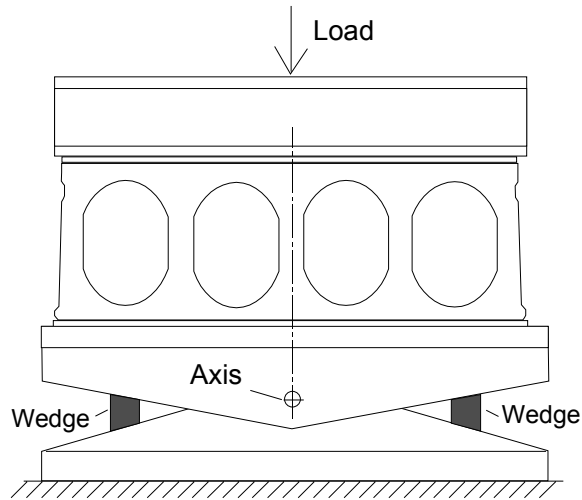


Figure 11. The wedges are loose when placing the slab into position to allow for initial longitudinal spirality. They are tightened before the test.

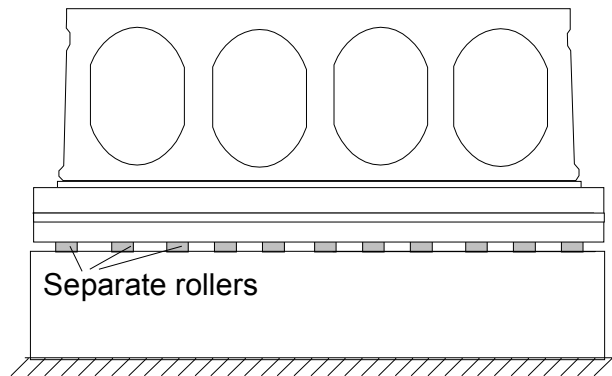


Figure 12. Separate rollers at passive end.

The measured geometrical and physical properties of the slabs, the failure modes and observed shear resistances, the date of loading as well as the date of casting, initial prestress and cross-sectional area of the strands given by the slab producer are given in Appendix C.

4. Analysis of test results

4.1 Assumptions

4.1.1 Material behaviour

All relevant provisions of EC2 have been followed as closely as possible when evaluating the material parameters. When simulating the tests, two approaches have been followed: that of EC2 [5] and that of Yang [10]. Since there is little knowledge about the concrete mix and storing conditions for the slabs, two values for the losses of prestress, 5% and 15%, are used. The aim is to show that the resistance is not sensitive to small variations in the losses and to provide an upper and a lower limit for the calculated resistance. The following assumptions have been made.

1. 50 mm core strength measured from six cores is the same as 150 mm cube strength. Characteristic strength is equal to mean strength – 1,645 times the standard deviation.
2. 150 mm cylinder strength f_{ck} is obtained from the cube strength according to EC2 by linear curve fitting between grades K45 and K85, i.e.

$$f_{ck,C150} = 0,8242f_{ck,K150} - 0,5156 \quad (14)$$

3. Mean (f_{ctm}) and characteristic value of tensile strength (f_{ctk}) are calculated from f_{ck} according to EC2, i. e.

$$f_{ctm} = 0,30 f_{ck}^{2/3} \quad \text{when } f_{ck} \leq 50 \text{ MPa} \quad (15)$$

$$f_{ctm} = (2,12 \text{ MPa}) \ln \left(1 + \frac{f_{ck,C150} + 8 \text{ MPa}}{10 \text{ MPa}} \right) \quad \text{when } f_{ck} > 50 \text{ MPa} \quad (16)$$

$$f_{ctk} = 0,70 f_{ctm} \quad (17)$$

4. $f_{ck}(28d)$ is calculated according to EC2 from f_{ck} , and f_{ck} at time of release is assumed to be = 70% of $f_{ck}(28d)$.
5. The stiffness of the tendons is taken into account when calculating the cross-sectional characteristics A , e , S and I . When doing so, $E_{c,28}$ and $E_p = 195 \text{ GPa}$ are used for the elasticity moduli of concrete and steel, respectively. Consequently,

the losses of prestress do not include the effect of elastic shortening due to the release of prestressing force. $E_{c,28}$ is obtained from

$$E_{c,28} = (22GPa) \ln \left(\frac{f_{ck}(28d) + 8MPa}{10MPa} \right)^{0,3} \quad (18)$$

6. The transfer lengths are calculated according to EC2 assuming gradual release (sawing), $\gamma_c = 1,5$ and good bond conditions except in few cases for upper strands.

According to EC2, the transfer length (basic value) is obtained from

$$l_{pt} = \alpha_1 \alpha_2 \phi \frac{\sigma_{pm0}}{\eta_{p1} \eta_1 f_{ctd}(t_{rel})} \quad (19)$$

where

α_1 is	1,00 (gradual release)
α_2	0,19 (7-wire strands)
ϕ	diameter of strand
σ_{pm0}	stress in tendon just after release
η_{p1}	3,2 (7-wire strand)
η_1	1,0 for lower strands and for upper strands in slabs not thicker than 265 mm
η_1	0,7 for upper strands in slabs with thickness 320 mm or more
t_{rel}	the age of the concrete at release.

It is assumed that at the release of the prestressing force, the strength of the concrete is 70% of the strength at 28 days. Applying EC2, 3.1.2 this results in

$$f_{ctd}(t_{rel}) = \frac{0,7 f_{ctm}(t_{rel})}{\gamma_c} = \frac{0,7 \cdot 0,7 f_{ctm}(28d)}{\gamma_c} = \frac{0,7 f_{ctk}(28d)}{\gamma_c} \quad (20)$$

It is strange that the expression for the basic value of the transfer length includes a safety factor $\gamma_c = 1,5$, but this seems to be made on purpose. Otherwise the safety factors 0,8 and 1,2 to be applied to the basic value in case of unfavourable and favourable effect of the prestressing, respectively, see [5], 8.10.2.2, do not make any sense.

4.1.2 Geometry

When calculating the characteristics of the concrete cross-section, the perimeter of the slab cross-section is assumed to be a rectangle, the depth of which is the nominal thickness of the slab and the width of which is the measured width of the slab at mid-depth. The nominal void geometry and position of the voids are used. On the other hand, the measured vertical position of the strands (mean value), the measured web width

$$b_w = \sum_i b_{w,i} \quad (21)$$

and the measured average slab weight are used for the stress analysis, see Figure 13.

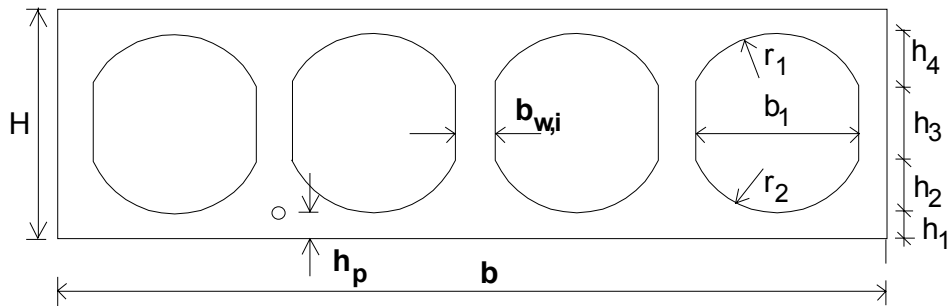


Figure 13. Geometrical model of slab cross-section in analysis. The measures printed in bold font are measured values, the other measures nominal ones.

For most geometrical parameters, the nominal geometry is used instead of measured geometry because

- the cross-sectional characteristics e , S/I and A , and hence the calculated stresses, are not sensitive to the measured small deviations from the nominal geometry. This is particularly true when the small errors due to these approximations are compared with other sources of error like transfer of prestressing force, tensile strength of concrete etc.
- the top surface of the slab is often curved, the real shape of voids does not correspond to any regular geometric figure, and a significant improvement in the accuracy would require much more sophisticated measurements and numerical analyses of results than those within the scope of the present project.

The measured web width b_w and position of the strands are used in the analysis because the results are sensitive to them. The measured average weight of the slabs and the width at the mid-depth of the section are also used because they can easily be measured. The measured slippage of the strands tell about the quality of compaction. Other measured parameters of the slab cross-sections, see Figure 8 and App. C, have been given to show that the use of nominal geometry in calculations is justified.

4.2 Comparison of predicted and observed resistance

The shear resistances calculated using both EC2 and Yang's method are given in the form of V_{obs}/V_{pre} in the following tables and figures. V_{obs} refers to the measured shear resistance (shear force at support) and V_{pre} is the corresponding predicted resistance calculated either according to EC2 or Yang. The absolute resistances, both observed and predicted ones, are given in Appendix C.

4.2.1 Predicted resistance calculated using mean tensile strength

Comparison of observed resistances with those calculated using the *mean tensile strength* is shown in Figure 14. For a perfect calculation model, the points would be on the straight line $V_{obs} = V_{pre}$, and for a good calculation model on both sides of the same line. This is clearly not the case for EC2 method which shows considerable nonconservatism. The fit for Yang's method is much better but not acceptable as such, either.

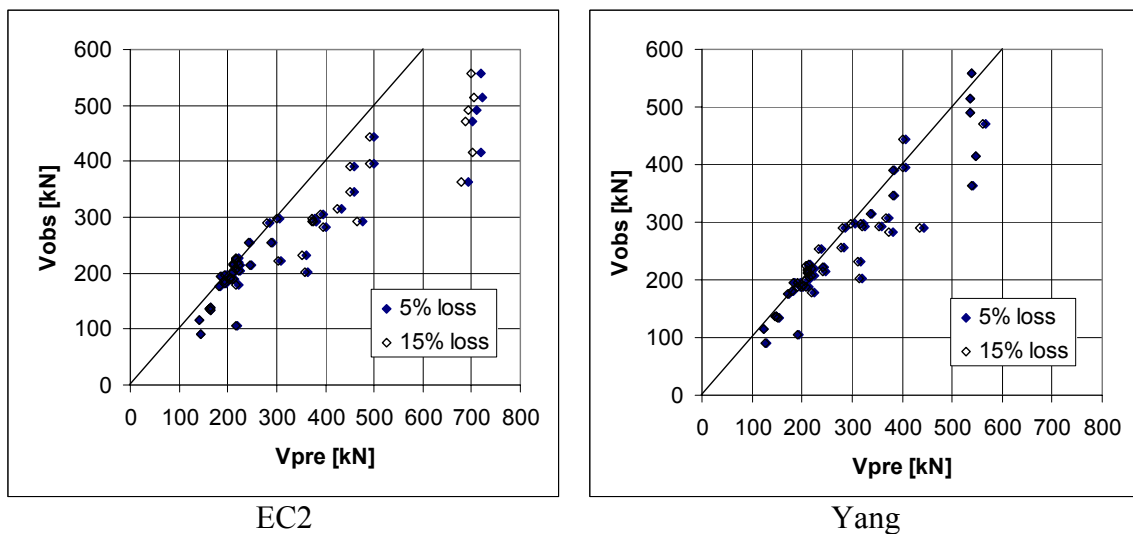
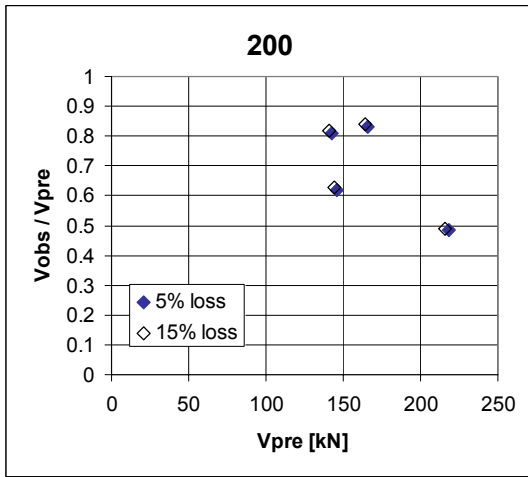
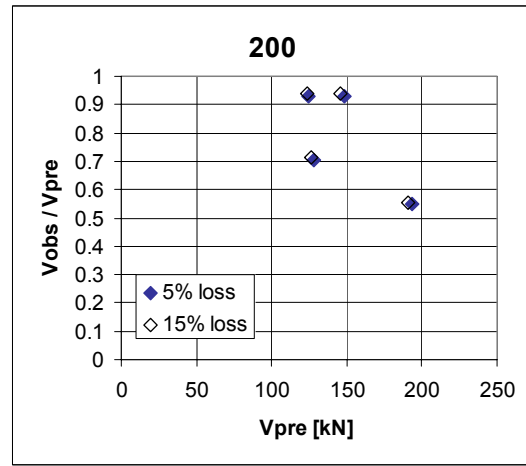


Figure 14. 200 mm slabs. Relationship of observed (V_{obs}) and predicted resistance (V_{pre}) calculated using mean tensile strength and the approach of EC2 and Yang.

To understand better the problem, different slab cross-sections are considered separately. The results are shown in Figures 15–20. For a valid calculation model, the mean of the ratios $\chi_i = V_{obs,i}/V_{pre,i}$ should be close to 1,0. This seems to be the case for 320 mm slabs with circular voids when calculated according to Yang. For 265 mm slabs (all with circular voids) both calculation methods give roughly the same result, the mean being slightly below 1,0. For other slab types Yang's approach gives a clearly better fit with test results than EC2, but seems still nonconservative, i.e. the mean is below 1,0. However, final conclusions should not be drawn from these comparisons, see 4.2.2.

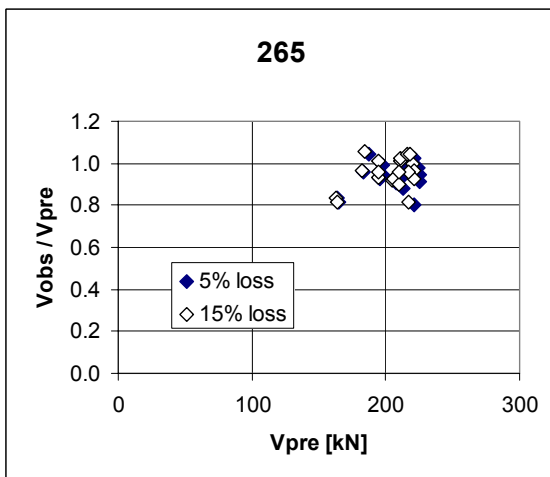


EC2

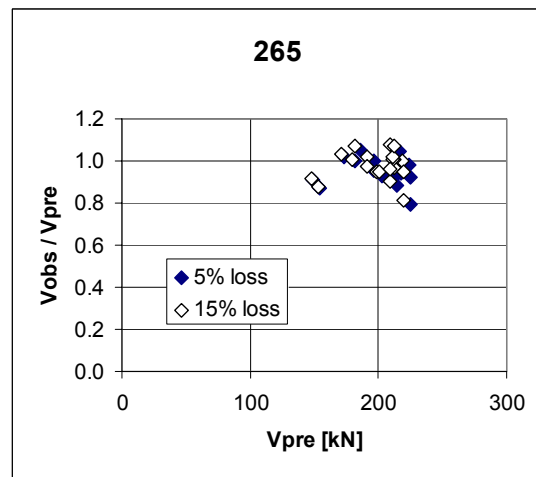


Yang

Figure 15. 200 mm slabs. Ratio of observed (V_{obs}) to predicted resistance (V_{pre}) calculated using mean tensile strength and the approach of EC2 and Yang.



EC2



Yang

Figure 16. 265 mm slabs. Ratio of observed (V_{obs}) to predicted resistance (V_{pre}) calculated using mean tensile strength and the approach of EC2 or Yang.

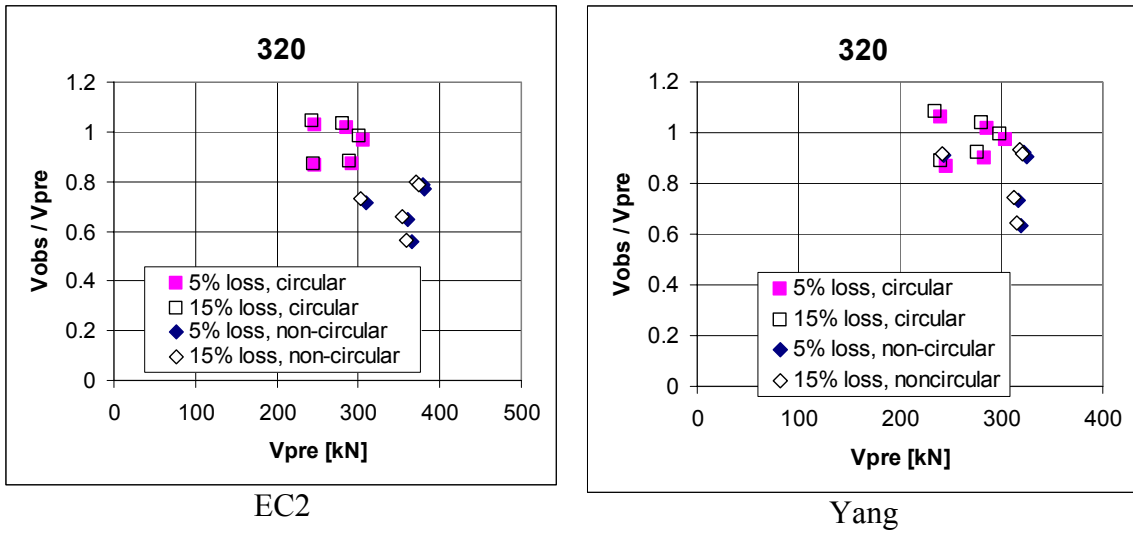


Figure 17. 320 mm slabs. Ratio of observed (V_{obs}) to predicted resistance (V_{pre}) calculated using mean tensile strength and the approach of EC2 or Yang.

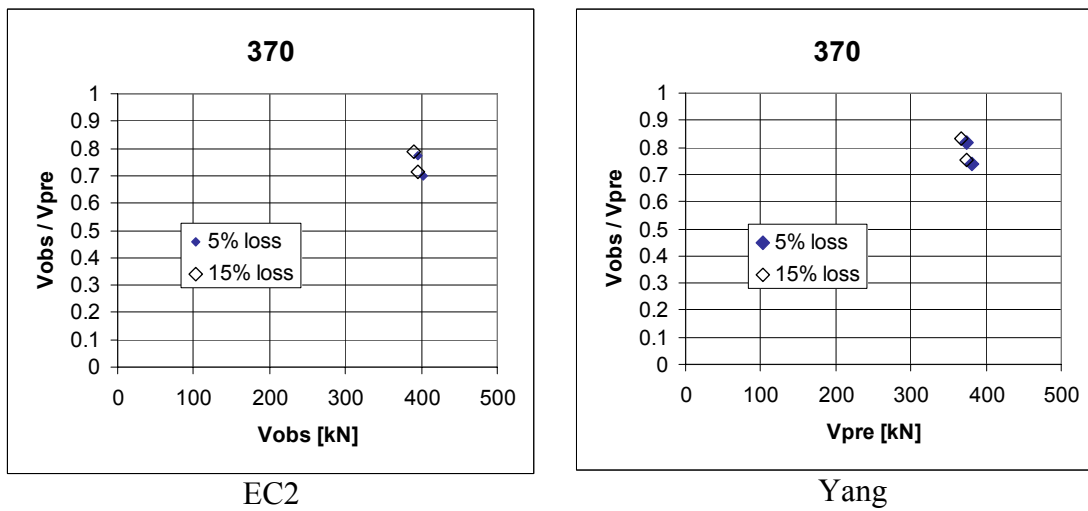


Figure 18. 370 mm slabs. Ratio of observed (V_{obs}) to predicted resistance (V_{pre}) calculated using mean tensile strength and the approach of EC2 and Yang.

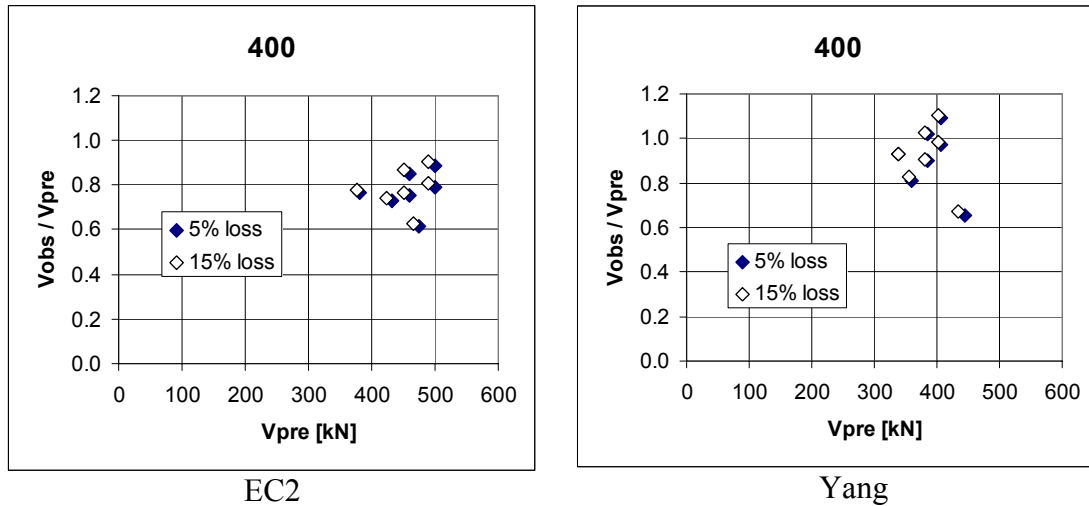


Figure 19. 400 mm slabs. Ratio of observed (V_{obs}) to predicted resistance (V_{pre}) calculated using mean tensile strength and the approach of EC2 and Yang.

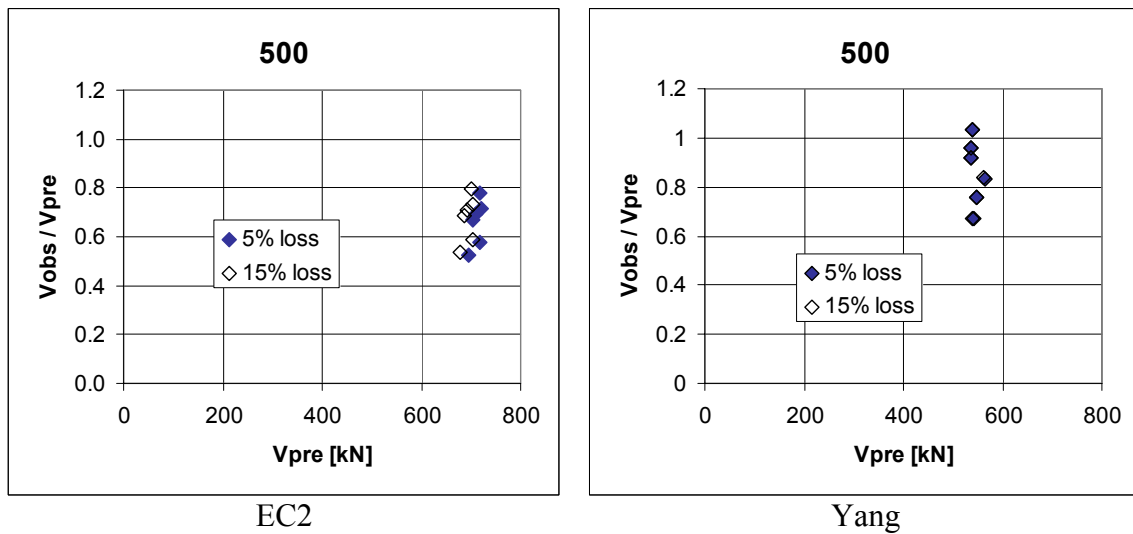


Figure 20. 500 mm slabs. Ratio of observed (V_{obs}) to predicted resistance (V_{pre}) calculated using mean tensile strength and the approach of EC2 and Yang.

4.2.2 Predicted resistance calculated using characteristic tensile strength

The design value of the shear resistance is calculated assuming that the characteristic tensile strength is 70% of the calculated mean tensile strength. This corresponds to variation coefficient 0,18 which may under- or overestimate the real behaviour. From the designer's point of view it is more important to know, whether a calculation model predicts the lower characteristic value of the shear resistance correctly. If this is the

case, and (fixed) safety factors are applied to the strength properties occurring in the model, we have all reasons to believe that the design value of the resistance, obtained from the model, is conservative enough.

Comparison of observed resistances with those calculated using *characteristic tensile strength* is illustrated in Figures 21–26. For a valid calculation model, at least 95% of the ratios $\chi_i = V_{obs,i}/V_{pre,i}$ should be above 1,0 and no more than 5% must be below 1,0. This seems to be the case for 320 mm slabs with circular voids and for 265 mm slabs (all with circular voids), but not for 200 mm slabs. For other cases the situation is not so clear. Therefore, for all slab thicknesses, the mean

$$\chi_{mean} = \frac{1}{n} \sum_{i=1}^n \chi_i \quad (22)$$

and the standard deviation

$$\chi_{stdev} = \sqrt{\frac{\sum_{i=1}^n (\chi_i - \chi_{mean})^2}{n-1}} \quad (23)$$

for the ratios $\chi_i = V_{obs,i}/V_{pre,i}$ are calculated. Assuming normal distribution, the 5% fractile $\chi_{5\%}$ is calculated from

$$\chi_{5\%} = \chi_{mean} - 1,645 \chi_{stdev} \quad (24)$$

From these expressions it can be deduced that if we write

$$\chi'_i = \frac{V_{obs,i}}{\chi_{5\%} V_{pre,i}} = \frac{1}{\chi_{5\%}} \frac{V_{obs,i}}{V_{pre,i}} \quad (25)$$

then

$$\chi'_{5\%} = \frac{1}{\chi_{5\%}} (\chi_{5\%}) = 1 \quad (26)$$

In other words, if $\chi_{5\%}$ is the 5% fractile of V_{obs}/V_{pre} , then the calculation model should be multiplied by $\chi_{5\%}$ to give the ideal resistance. In this sense $\chi_{5\%}$ is a calibration factor and a measure for the accuracy of the calculation model. The original calculation model is overconservative or nonconservative depending on whether $\chi_{5\%}$ is greater or smaller than 1,0, respectively. The obtained $\chi_{5\%}$ -factors for different slab types, given in Table 6, represent the mean of two $\chi_{5\%}$ values, calculated using 5% and 15% loss of prestress.

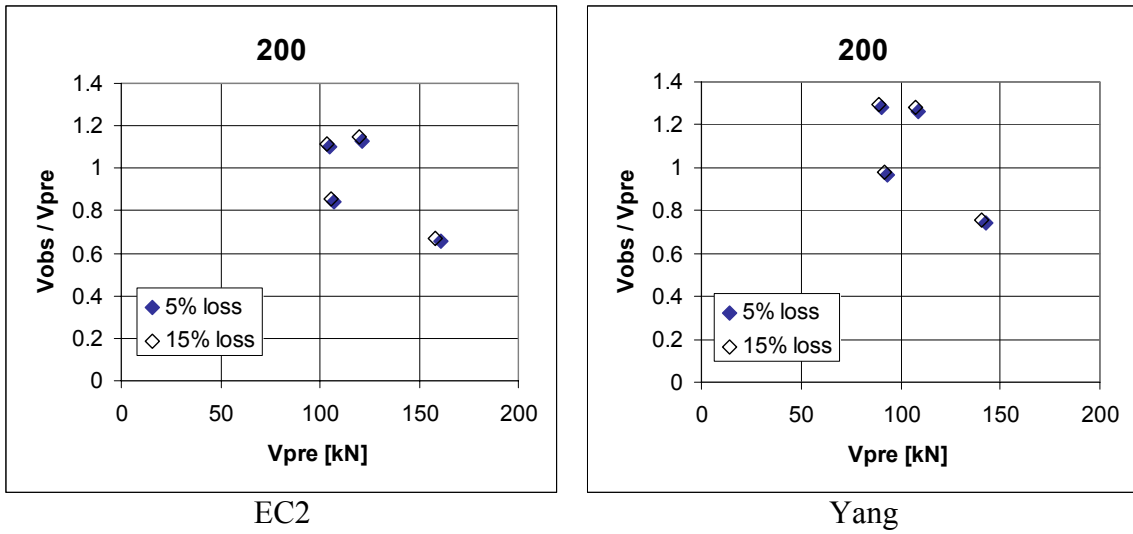


Figure 21. 200 mm slabs. Ratio of observed (V_{obs}) to predicted resistance (V_{pre}) calculated using characteristic tensile strength and the approach of EC2 and Yang.

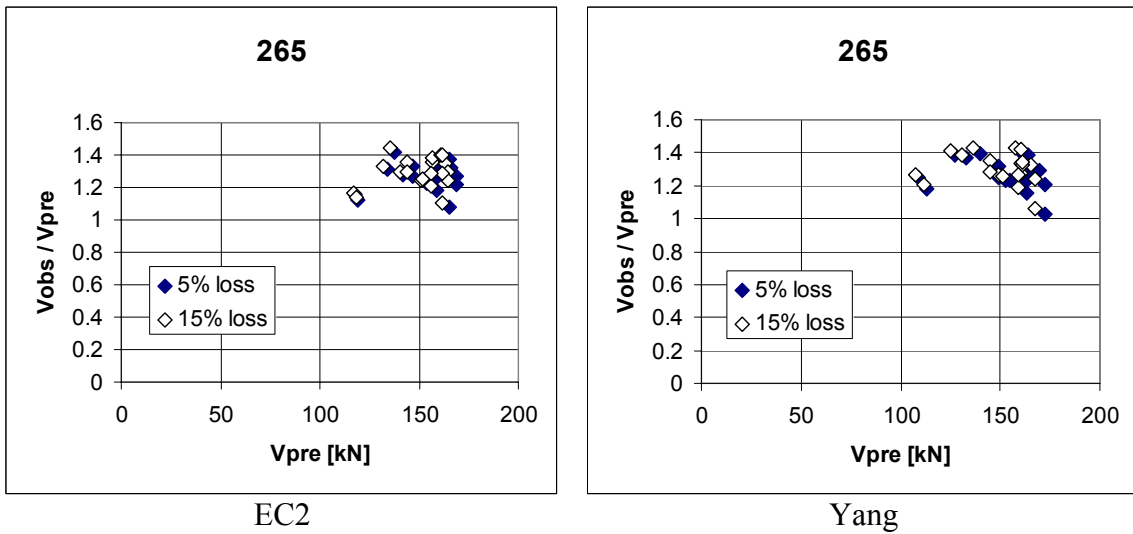


Figure 22. 265 mm slabs. Ratio of observed (V_{obs}) to predicted resistance (V_{pre}) calculated using characteristic tensile strength and the approach of EC2 and Yang.

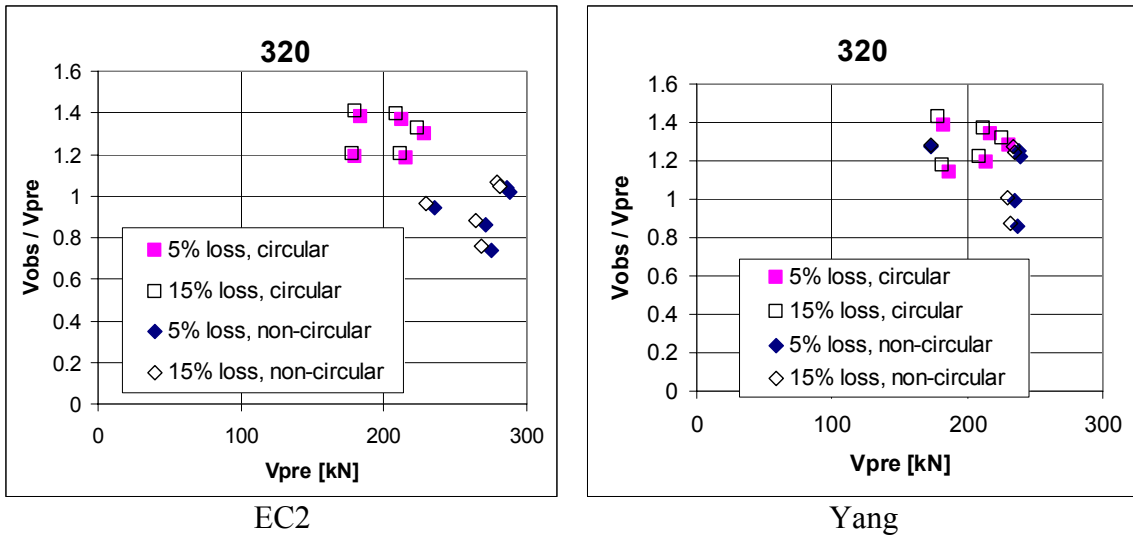


Figure 23. 320 mm slabs. Ratio of observed (V_{obs}) to predicted resistance (V_{pre}) calculated using characteristic tensile strength and the approach of EC2 and Yang.

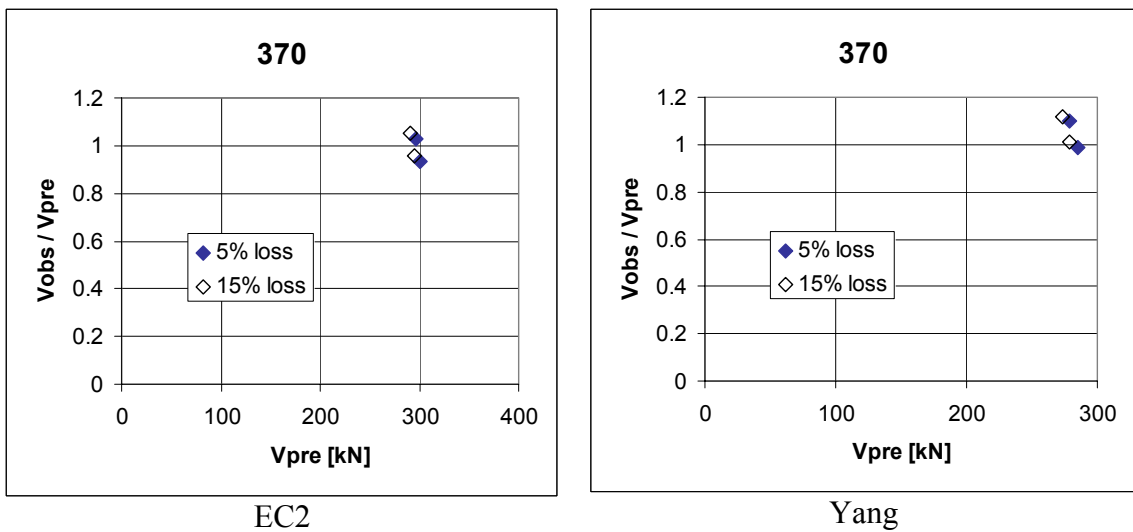


Figure 24. 370 mm slabs. Ratio of observed (V_{obs}) to predicted resistance (V_{pre}) calculated using characteristic tensile strength and the approach of EC2 and Yang.

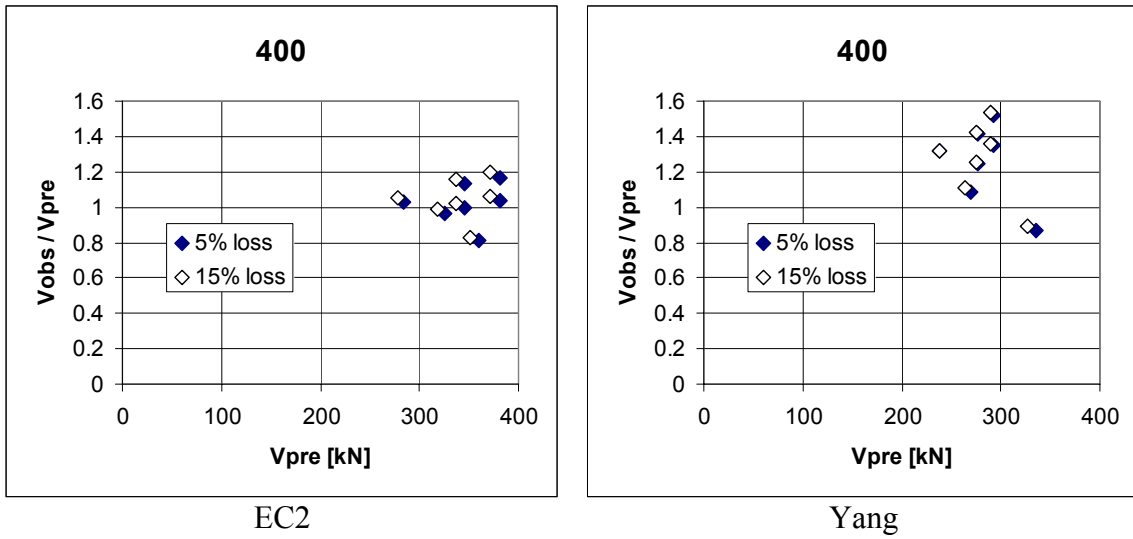


Figure 25. 400 mm slabs. Ratio of observed (V_{obs}) to predicted resistance (V_{pre}) calculated using characteristic tensile strength and the approach of EC2 and Yang.

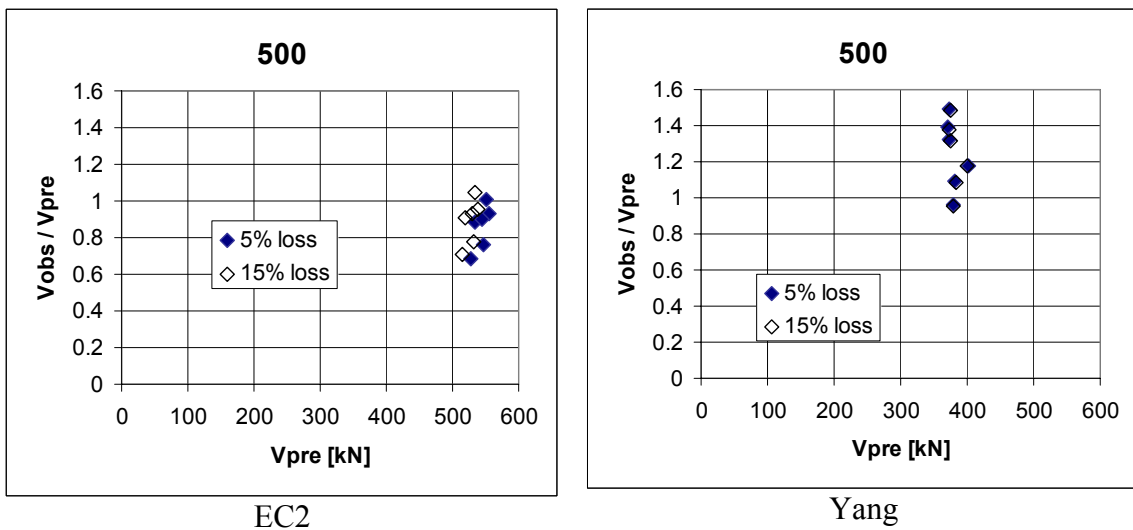


Figure 26. 500 mm slabs. Ratio of observed (V_{obs}) to predicted resistance (V_{pre}) calculated using characteristic tensile strength and the approach of EC2 and Yang.

Table 6. Calibration factors for different slab groups when using EC2 ($\chi_{5\%,EC2}$) and Yang's method ($\chi_{5\%,Yang}$).

Slab thickness mm	Number of tests	$\chi_{5\%,EC2}$	$\chi_{5\%,Yang}$
200	4	0,57 ¹⁾	0,64 ²⁾
265	20	1,13	1,14
320 (All)	10	0,75	0,94
320 (Circular)	5	1,14	1,12
320 (Non-circular)	5	0,72 ³⁾	0,82 ⁴⁾
370	2	-	-
400	7	0,84	0,92
500	6	0,68	0,91
400 + 500	13	0,73	0,93
320–500 with non-circular voids	18	0,75	0,88
All	49	0,79	0,96

¹⁾ Eliminating one test result (40.200) would give 0,77 here

²⁾ Eliminating one test result (40.200) would give 0,89 here.

³⁾ Eliminating one test result (517.320) would give 0,84 here.

⁴⁾ Eliminating one test result (517.320) would give 0,98 here.

The number of tests on 200 mm slabs is small and the scatter in the results exceptionally high when compared with other slab types. In Table 7 the present test results are compared with some old test results on similar 200 mm slabs [8]. All slabs in Table 7 were prestressed with seven strands, each with 12,5 mm diameter and cross-sectional area of 93 mm². The old tests comprise all such test specimens from [8] meeting at least one of the criteria: either observed or predicted failure mode had to be shear tension failure of web. This means that in the old tests, the real resistance against shear tension failure was at least as high as that given in Table 7.

Table 7 shows that the resistance observed in the old tests is on a considerably higher level than in the present tests. The difference is so clear, particularly for slab 40.200, that it cannot be explained by differences in the strength or geometric parameters. Excluding this test would result in tens of percent improvement in $\chi_{5\%}$. Therefore, and because the number of the present tests is small (4), no serious conclusions should be drawn from this study on 200 mm slabs.

A similar conclusion seems justified for 320 mm slabs with non-circular voids: there are three slabs at a higher level, and two slabs at a considerably lower level. Eliminating the lowest point has again a strong effect on $\chi_{5\%}$. For 400 mm slabs there is also one point clearly below the others, but due to the greater number of points, one point has a minor effect on the result.

Table 7. 200 mm slabs. Observed shear resistance V_{obs} , observed failure mode FM_{obs} , predicted failure mode FM_{pre} , initial prestress σ_{p0} , characteristic core strength $f_{ck,C50}$ and measured web width b_w in the present and in some old tests [8].

	Slab	V_{obs} kN	$FM_{obs}^{1)}$	$FM_{pre}^{1)}$	σ_{p0} MPa	$f_{ck,C50}$ MPa	b_w MPa
Present tests	31.200	90	ST	ST	1100	48,5	239
	33.200	116	ST	ST	1100	47,5	238
	40.200	106	ST	ST	1100	70,2	293
	63.200	137	S	ST	1000	52,5	262
Old tests	44.2	>193	Interr.	ST	1100	48,8	242
	51.2	135	S	SA	100	50,8	236
	56.2	140	S	F	900	51,7	266
	59.2	>148	SII	ST	1000	51,6	248
	67.2	121	S	ST	1100	70,9	242

ST Shear tension failure in web

S Shear failure (no more data in test report, but in practice the same as ST)

SII Shear failure between the first and second transverse line load

SA Anchorage failure between support and first transverse line load

Interr. Test interrupted due to excessive deflection

F Flexural failure

For 265 mm slabs there seems to be no major difference in the results depending on the calculation model. Both models seem to give slightly overconservative results.

The slabs with thickness 320 mm can be divided into two categories: those with circular voids and those with non-circular voids. The slabs with circular voids are safely designed using either of the models, but EC2 gives somewhat more overconservative results than Yang's method. On the other hand, both methods give nonconservative results for slabs with noncircular voids, but Yang's method gives a better fit with test results.

For 370 mm slabs Yang's method gives a safer prediction than EC2, but no statistical evaluation is possible based on two test results only.

For 400 mm and 500 mm slabs Yang's method gives a considerably better fit with test results than EC2, but is still 8% and 9%, respectively, on the unsafe side. For 500 mm slabs and EC2 method, the fit with test results is poor.

When all slabs with noncircular voids are considered, EC2 and Yang's method give $\chi_{5\%}$ equal to 0,75 and 0,88, respectively. Generally speaking, EC2 and Yang's method are equal for 265 mm slabs, but for all other slab types and thicknesses Yang's method gives a significantly better fit with the experimental results.

One way to enhance the safety of EC2 method is to use a lower tensile strength. E.g. in CEB Bulletin 228 [2] the tensile strength is calculated from

$$f_{ctm} = 0,3178MPa \left(\frac{f_{ck,C150} + 8MPa}{1MPa} \right)^{0,6} \quad (27)$$

In Figure 27 this is compared with the tensile strength calculated according to EC2.

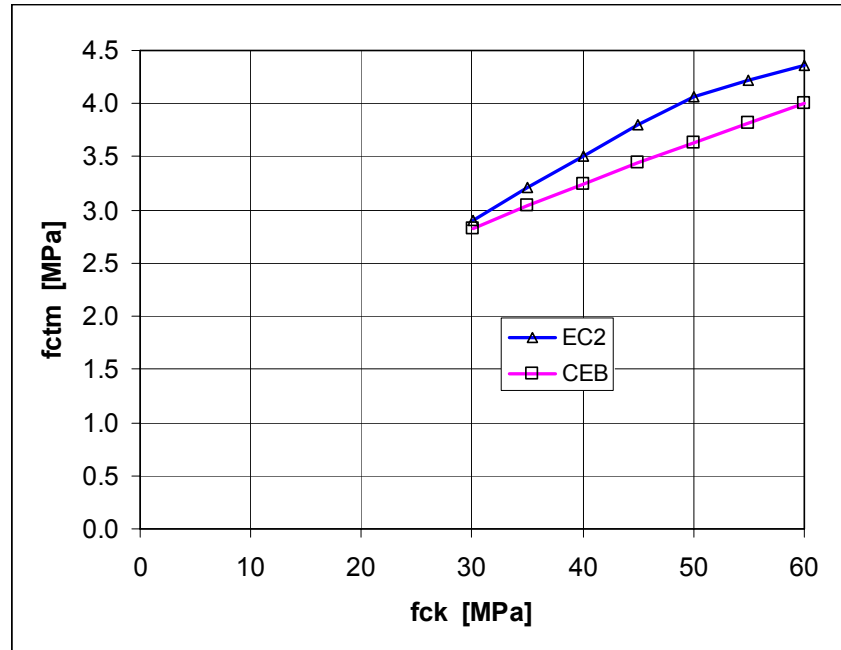


Figure 27. Comparison of mean tensile strength calculated according to EC2 and CEB Bulletin 228.

The calibration factors calculated using CEB strength in EC2 method and the calibration factors from Table 6 are compared in Figure 28. The reduction of tensile strength reduces the calculated shear resistance in all cases, also for 265 mm slabs and for 320 mm slabs with circular voids for which there is no need for reduction. The fit remains worse than with Yang's method for all slab groups. It is obvious that reducing the value of the tensile strength in the calculation model is no solution to improve the fit even though the safety level can be enhanced in this way.

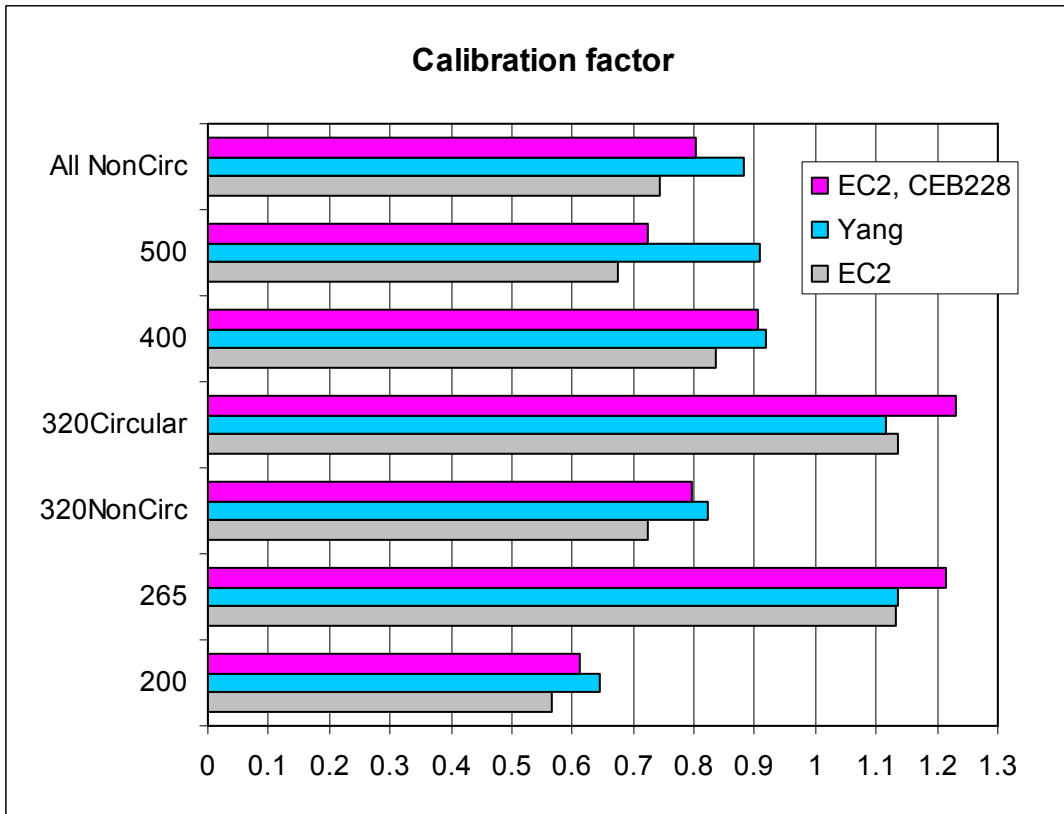


Figure 28. Calibration factor ($\chi_{5\%}$) needed to make the predicted resistance equal to the observed resistance when using EC2 method, Yang's method and modified EC2 method applying reduced tensile strength (EC2, CEB228).

4.2.3 Location of critical point

The location of the critical point is easily determined in EC2 method. The longitudinal location is fixed and the vertical position is the one where $S/(Ib_w)$ has its highest value. This is the centroidal axis, if the web is thinnest there. For slabs with circular voids the critical point is at the axis going through the centroids of the voids or close to it.

When using Yang's method, the location of the critical point in the web is not self-evident. However, for slabs with circular voids, the critical point cannot be far from the centroidal axis of the voids. For slabs with non-circular voids the position has to be determined case by case. If the webs are flat, a good guess for the critical position is the junction of the webs and the flange.

As an example, the shear resistance calculated according to Yang, corresponding to the failure criterion (Eq.1) at different depths, is illustrated in Figures 29 and 30 for two test specimens. Note that all considered points lie on an inclined line (line A'-B' in Figure 6.b). The critical point for the 265 mm slab (Figure 29) is slightly below the mid-depth

where the web width is thinnest, that for the 400 mm slab slightly below the junction of the flat web and the bottom flange, see also Figures 30 and 31.

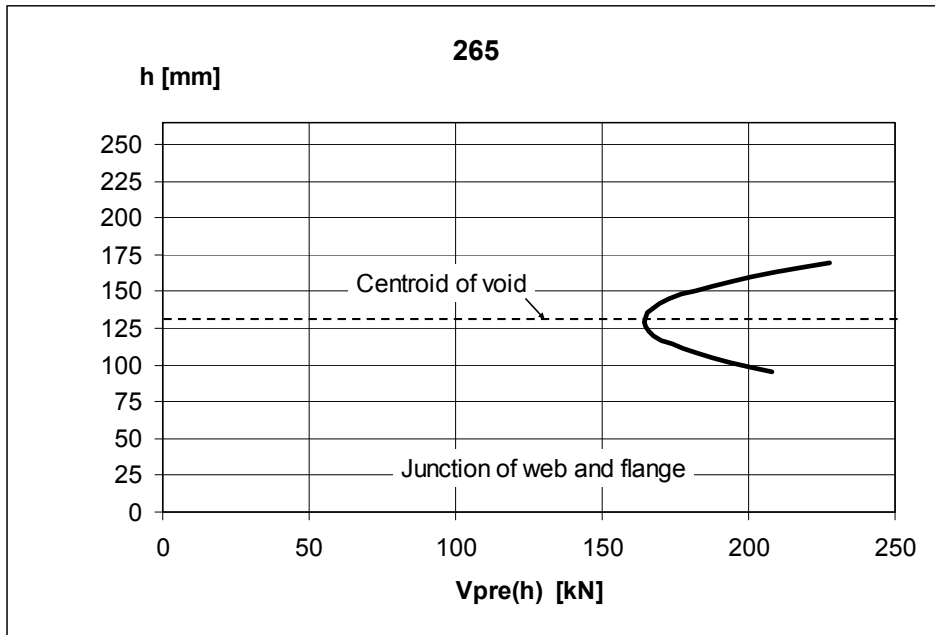


Figure 29. Slab 512.265, Yang's method. Characteristic value of shear resistance corresponding to failure criterion at different depths h .

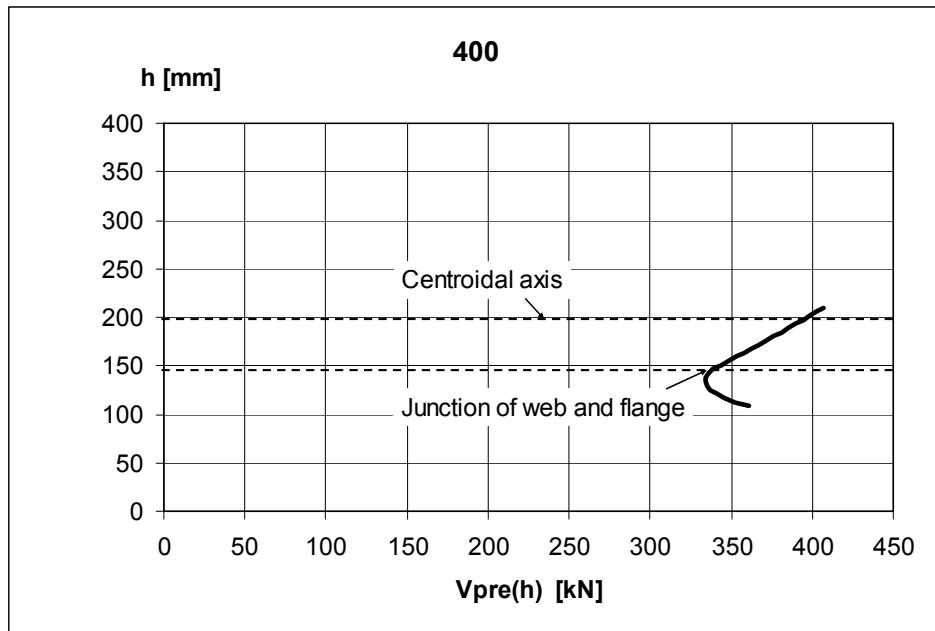


Figure 30. Slab 178.400, Yang's method. Characteristic value of shear resistance corresponding to failure criterion at different depths h .

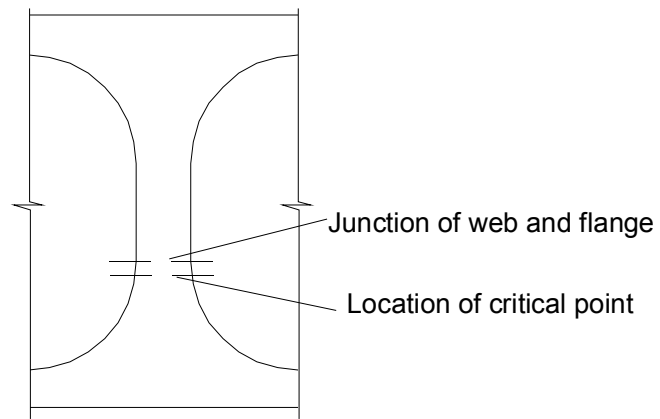


Figure 31. Slab 178.400, Yang's method. Location of critical point.

5. Discussion

5.1 Assessment of tests

The tests, the results of which have been analysed here, have served for different purposes. They comprise

- two quality control tests or QC tests (40.200 and 162.400)
- 21 tests carried out in research projects or RP tests (those of the type 500.xyz)
- 26 type approval tests or TA tests.

The quality control tests represent the normal production from which a third party has chosen the test specimens. Despite the great number of QC tests carried out in Finland, there are only two tests belonging to this category in the approved 49 tests. The reasons for this are as follows

the failure mode has not been the web shear failure (thin slabs, long slabs and slabs with a small number of strands)

- the shear span has been shorter than 2,4 times the slab thickness (thick and short slabs)
- in the vast majority of the quality control tests carried out in Finland neither the strength of the concrete nor the web width have been measured, which makes all such test useless for the present purpose.

Type approval tests have been performed when a new producer or a new factory has been starting production or when a new slab type has been introduced in an old factory. Sometimes it has happened that the results of the first TA tests suggest that there is something wrong in the compaction, concrete mix or somewhere else. After tuning the production method, a new test series has been performed showing enhanced shear resistance. Since all type approval tests are included, there is a tendency that the resistances observed in the TA tests are at a lower level than those from QC tests and the scatter is larger.

The test specimens in the third type of tests, RP tests, are likely to present the best quality of normal production. The producer has often paid special attention to the inspection of these specimens in order not to jeopardize an expensive research project. In some cases the producer has checked experimentally the shear resistance of the slabs before transporting them to the research laboratory.

Due to the small number of tests, no statistical evaluation of the differences between the type approval tests and research project tests is justified. However, it is likely that in

a continuous production it is possible to achieve on an average a slightly higher shear resistance than that observed in the present tests.

5.2 Results from other researchers

Fellinger [6] has analysed a great number of shear tests on prestressed hollow core slabs to check the validity of EC2 method much in the same way as has been done here. His test data have been collected from many sources and from many countries. In many cases he has been obliged to evaluate some parameters because they have not been recorded. He has considered all test results as one population, calculated the ratio $\chi_i = V_{obs,i}/V_{pre,i}$ for all tests i , and got a mean equal to 0,92. From this he has concluded that “... there is no need to modify the model since there is a very large margin between the mean model value and the design value ranging from 1,5 for lower strength up to 2,5 for higher strengths.” He has confirmed this conclusion by the observation that the accuracy of the model is almost independent of the parameters it includes.

However, the accuracy of the model seems to be strongly and systematically dependent on the slab cross-section. This is illustrated in Table 8 in which different subsets of the whole population are considered separately.

Table 8. Mean value of ratios of observed shear resistance to predicted shear resistance.

Slab thickness [mm]	All	265	370–400	500
Yang (FIP [7])	0,92	1,13	0,86	-
Fellinger (EC2)	0,92		0,87*)	-
Present study (EC2)	0,83	0,95	0,77	0,67

*) Excluding four tests would give 0,84 here. In these four tests (PC400-1, PC400-2, ST400-1, ST400-2) the loaded slab ends were provided with transversally reinforced cast-in-situ concrete extending 50 mm into the voids and 50 mm outside the slab ends.

Table 8 shows that there is the same trend in all results. It also illustrates why a calculation model cannot be verified by considering the effect of the parameters included in the model only. It is equally important to verify that all essential parameters are included. In this case, the shear resistance of 265 mm slabs with circular or oval voids is not affected by the transfer of the prestressing force but for slabs with flat webs the transfer must not be ignored. The effect of the shape of the webs on the shear resistance is so strong that regarding all slabs as one population is not justified.

5.3 Mean or characteristic resistance?

When calibrating resistance models, the basic idea is to compare the test results with the theoretical resistances calculated from the measured parameters of the test specimens. When doing so, the mean value of the strength, elasticity modulus etc. is used.

If a calculation model is perfect, it predicts the mean shear resistance when using the mean strength values and the characteristic shear resistance when using the characteristic strength values. Both EC2 model and Yang's model predict the characteristic shear resistance more accurately than the mean resistance, i.e., the underconservatism observed for the slabs with flat webs is clearly smaller when the characteristic shear resistance is considered. This is obviously due to the intrinsic conservatism in the assumption that the characteristic tensile strength is as low as 70% of the mean tensile strength. Since the characteristic shear resistance, not the mean one, is the value manipulated by safety factors when the design resistance is searched for, it should be enough to show that the calculation model correctly predicts the characteristic resistance. This simply means that the characteristic value of the test results should be no less than the predicted resistance calculated using the characteristic strength.

5.4 Comparison of EC2 vs. Yang's method

The method of EC2 seems to give ambiguous results. For 265 and 320 mm slabs with circular voids it seems to give reasonable, even though a bit overconservative results. On the other hand, the results for slabs with flat webs are too much on the unsafe side to be explained by some errors in the test arrangements or defects in the tested slabs. Yang's method gives a considerably better fit with the test results than EC2 method, particularly for those slabs for which the EC2 method gives the most unsafe results. However, the predictions of Yang's method are not in all cases on the safe side, either. Reasons for this may be that the type approval tests, see 5.1. do not represent the quality of the normal production or that the tensile strength in the top flange, where the cores have been drilled, differs from that in the web where the tensile strength should be determined.

As a whole, Yang's method means such an improvement on the accuracy that it should replace the existing method in EC2.

6. Summary and conclusions

Eq. 6.4 in EC2 presents a design method for the shear resistance of webs in members which have no shear reinforcement. This method is widely used for prestressed hollow core slabs. To check the validity of the method, 49 shear tests on hollow core slabs with thickness 200–500 mm have been analysed. All tests ended with a web shear tension failure.

The EC2 method overestimated the mean shear resistance of all tested slab types. The mean shear resistance of 265 mm or 320 mm slabs with circular voids was slightly overestimated, but the resistance of 200 mm slabs and slabs with flat webs by tens of percent. When the characteristic experimental resistances were compared with the calculated characteristic resistance, the fit was better but there was still a considerable lack of safety for 200 mm slabs and for the slabs with flat webs. On the other hand, the EC2 method was (over)conservative for 265 mm and 320 mm slabs with circular voids.

The EC2 method ignores the shear stresses due to the transfer of the prestressing force. When these stresses were taken into account applying Yang's method, the accuracy for 265 mm and 320 mm slabs with circular voids was the same as when using EC2 method but much better for the other slabs.

The predicted shear resistances may be reduced by reducing the tensile strength from that specified in EC2 e.g. to that given in CEB bulletin 228 [2]. This modification improved the fit of EC2 method with test results for those slabs for which the observed resistance was too low, but it also reduced the predicted resistance for the slabs for which there was no need for such a reduction. Furthermore, when considering the characteristic resistances, the fit with test results of the modified EC2 method using a lower tensile strength was still worse for all slab types than with Yang's method applied without any reduction of tensile strength.

The fit of Yang's method was poorest for 200 mm slabs and 320 mm slabs with flat webs, which is mainly attributable to one poor test results in both cases. The elimination of the poorest test result from the test data enhanced the observed characteristic resistance considerably. When this was done, the characteristic resistance calculated according to Yang's method was 89–98% of the experimental characteristic resistance for the problematic cases, i.e. for 200 mm slabs and slabs with flat webs. For comparison, the corresponding figures for EC2 method were 68–84%, the lowest value being for 500 mm slabs. For nonproblematic cases both methods were equal and gave conservative results.

Based on the results, Yang's method for design against web shear failure should replace the present method, i.e. Eq. 6.4 in EC2, because it gives a much better fit with test results and because it is theoretically more correct. It is not acceptable, however, to adopt a design method which overestimates the characteristic resistance of some product type by 10% as Yang's method seems to do. Whether this is really the case, is still an open question because the number of tests on the problematic slabs was small, and due to the nature of the type approval tests, some test specimens may have been weaker than the slabs typical of normal production. This question can be answered by carrying out a series of tests on the slab types most susceptible to the shear stresses due to the transfer of the prestressing force. Another way would be to modify the shear resistance calculated according to Yang's method by a reduction factor of the order of 0,90 except for slabs with circular or oval voids for which the method could be used without modification.

The EC2 method (Eq. 6.4) should never be used without a reduction factor for slabs with flat webs, and its applicability to other slab types should always be verified either numerically or experimentally before it is used.

References

1. *BBK 79 Bestämmelser för betongkonstruktioner, Band 1, Konstruktion*. Stockholm: Statens betongkommitté, 1979. 157 p. ISBN: 91-7332-087-0.
2. CEB Bulletin 228. *High Performance Concrete – Recommended Extensions to the Model Code 90 – Research Needs, 1995*. Comité Euro-International du Béton. 60 p. ISBN: 2-88394-031-2/1995.
3. *CPI100: Part 1: November 1972. Code of practice for the structural use of concrete*. London: British Standards Institution, November 1972. ISBN: 0 580 07488 9.
4. EN 1168. *Precast concrete products – Hollow core slabs*. 2005.
5. EN 1992-1-1. *Eurocode 2: Design of concrete structures – Part 1: General rules and rules for buildings*. 2004.
6. Fellingner, J. *Shear and anchorage behaviour of fire exposed hollow core slabs*. Delft: Delft University Press, 2004. 234 p. + app. 26 p. ISBN: 90-407-2482-2.
7. FIP Recommendations "*Precast prestressed hollow core floors*". London: Thomas Telford, 1988. 31 p. ISBN: 0 7277 1375 2.
8. Pajari, M. *Design of prestressed hollow core slabs*. Espoo: Technical Research Centre of Finland, 1989. Research Reports 657. 88 p. + app. 38 p. ISBN 951-38-3539-1.
9. Walraven, J. C. & Merx, W. P. M. *The bearing capacity of prestressed hollow core slabs*. Heron 1983. Vol. 28, No. 3. 46 p.
10. Yang, L. *Design of Prestressed Hollow core Slabs with Reference to Web Shear Failure*. ASCE Journal of Structural Engineering, 1994. Vol. 120, No. 9, pp. 2675–2696.

Appendix A: Expression for shear stress

Yang derived his shear formula for a case with no strands above the considered horizontal plane. He considered the horizontal equilibrium for the free body diagram shown in Figure 1.

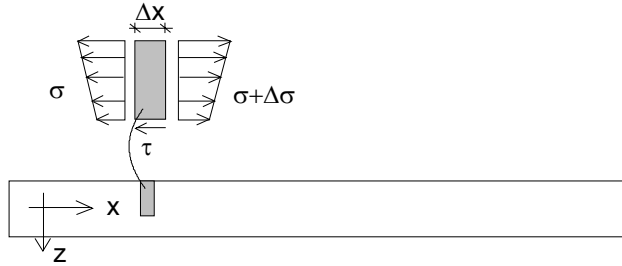


Figure 1. Free body diagram for slabs without upper tendons.

From the equilibrium of forces on the free body shown in Figure 1

$$tb\Delta x \approx \int_{A_{cp}} (\Delta\sigma) dA \quad \text{or} \quad \tau = \frac{1}{b_w} \int_{A_{cp}} \frac{d\sigma}{dx} dA \quad (1)$$

where σ denotes the axial stress in the concrete, b_w the width of the web at the considered horizontal axis and A_{cp} the cross-sectional area above the considered axis.

In a more more general case there are tendons above the considered axis. In this case the equilibrium of forces acting on the free body shown in Figure 2 gives

$$tb\Delta x \approx \int_{A_{cp}} (\Delta\sigma) dA + \Delta P \quad \text{or} \quad \tau = \frac{1}{b_w} \int_{A_{cp}} \frac{d\sigma}{dx} dA + \frac{1}{b_w} \frac{dP}{dx} \quad (2)$$

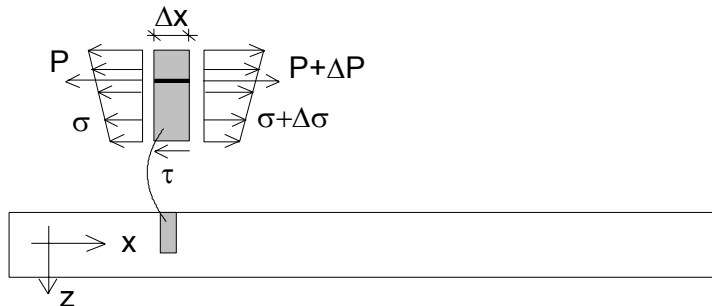


Figure 2. Free body diagram for a slab with upper tendons.

If there are n layers of prestressing tendons, the axial stress s is obtained from the well-known expression

$$\sigma = \frac{-\sum_{i=1}^n P_i}{A} + \frac{-\sum_{i=1}^n P_i e_i + M}{I} z \quad (3)$$

where P_i is the prestressing force in the tendon layer i (positive), e_i its eccentricity (positive below centroidal axis, negative above it), A the cross-sectional area and I the second moment of area of the cross-section. A straight-forward differentiation of Eq. 3 gives

$$\begin{aligned} \frac{d\sigma}{dx} &= -\frac{1}{A} \sum_i \frac{dP_i}{dx} + \frac{-\sum_i e_i \frac{dP_i}{dx} + \frac{dM}{dx}}{I} z \\ &= -\frac{1}{A} \sum_i \frac{dP_i}{dx} + \frac{z}{I} \sum_i e_i \frac{dP_i}{dx} + \frac{z}{I} V \end{aligned} \quad (4)$$

Substituting this in Eq. 2 and writing (mere notation)

$$S_{cp} = - \int_{A_{cp}} z dA \quad (5)$$

gives

$$\tau = -\frac{1}{b} \left[\frac{A_{cp}}{A} \sum_{i=1}^n \frac{dP_i}{dx} - \frac{S_{cp}}{I} \sum_{i=1}^n e_i \frac{dP_i}{dx} + \frac{S_{cp}}{I} V - \sum_j \frac{dP_j}{dx} \right] \quad (6)$$

where A_{cp} is the cross-sectional area above the axis at which τ is considered and $\sum_j \frac{dP_j}{dx}$

represents the sum of all tendon force gradients above the considered axis. If there is only one tendon layer at the bottom of the cross-section, Eq. 6 reduces to

$$\tau = -\frac{1}{b} \left[\left(\frac{A_{cp}}{A} - \frac{S_{cp} e}{I} \right) \frac{dP}{dx} + \frac{S_{cp}}{I} V \right] \quad (7)$$

which is the expression presented by Yang.

Reversing the sense of τ in Figures 1 and 2 the minus sign on the right hand side of Eqs 6 and 7 may be omitted.

Appendix B: Criterion for bond slip

At a sawn slab end, bond slip is measured for each strand. The following requirements shall be fulfilled

$$\text{Individual slip} \leq 1,3\Delta l_0$$

$$\text{Mean slip} \leq \Delta l_0$$

$\Delta l_0 = \varepsilon_p d$ where ε_p is the strain of the strand before the release and d the diameter of the strand.

Appendix C: Data about tests

Table 1. Test type, slab type, nominal depth of slab (H), number of upper strands (N_{up}), diameter of an upper strand (D_{up}), cross-sectional area of an upper strand (A_{up}), initial prestress in upper strands ($\sigma_{p0,up}$) and the corresponding characteristics for the lower strands (N_{low} , D_{low} , A_{low} , $\sigma_{p0,low}$).

Test	Test type	Slab type	H mm	N_{up}	D_{up} mm	A_{up} mm ²	$\sigma_{p0,up}$ MPa	N_{low}	D_{low} mm	A_{low} mm ²	$\sigma_{p0,low}$ MPa
31.200	1	602	200					7	12,5	93	1100
33.200	1	602	200					7	12,5	93	1100
40.200	1	601	200					7	12,5	93	1100
63.200	1	601	200					7	12,5	93	1000
74.265	1	501	265					5	12,5	93	1100
98.265	1	501	265					10	12,5	93	1100
104.265	1	501	265					4	12,5	93	1000
107.265	1	501	265					4	12,5	93	1000
109.265	1	501	265					10	12,5	93	1000
110.265	1	502	265					8	12,5	93	1000
113.265	1	502	265	2	9,3	52	900	4	12,5	93	1000
114.265	1	502	265	2	9,3	52	900	8	12,5	93	900
115.265	1	502	265					6	12,5	93	1000
116.265	4	501	265					6	12,5	93	1100
501.265	5	501	265	0				10	12,5	93	1100
502.265	5	501	265	0				10	12,5	93	1100
503.265	5	501	265	0				10	12,5	93	950
504.265	5	501	265	0				10	12,5	93	950
505.265	5	501	265	0				10	12,5	93	950
506.265	5	501	265	0				10	12,5	93	950
507.265	5	501	265	0				10	12,5	93	950
508.265	5	501	265	0				10	12,5	93	950
509.265	5	501	265	0				10	12,5	93	950
510.265	5	501	265	0				10	12,5	93	950
511.265	5	501	265	0				10	12,5	93	950
512.265	5	501	265	0				10	12,5	93	950
132.320	3	503	320					10	12,5	93	1100
133.320	3	503	320					12	12,5	93	1100
134.320	3	503	320					12	12,5	93	1100
136.320	4	410	320					4	12,5	93	1000
138.320	4	410	320					13	12,5	93	1000
139.320	4	410	320					7	12,5	93	1000
146.320	1	401	320					6	12,5	93	1000
148.320	1	401	320	2	9,3	52	900	11	12,5	93	1000
151.320	1	401	320					9	12,5	93	950
513.320	5	421	320	2	12,5	93	900	13	12,5	93	1100
514.320	5	411	320	0				13	12,5	93	1100
515.320	5	411	320	0				13	12,5	93	1100
516.320	5	421	320	0				11	12,5	93	1000
517.320	5	421	320	0				11	12,5	93	1000

Table 1. Continued.

Test	Test type	Slab type	H mm	N_{up}	D_{up} mm	A_{up} mm ²	$\sigma_{p0,up}$ MPa	N_{low}	D_{low} mm	A_{low} mm ²	$\sigma_{p0,low}$ MPa
159.370	3	412	370					10	12,5	93	1000
160.370	3	412	370					12	12,5	93	1000
161.370	3	412	370					12	12,5	93	1000
162.400	1	415	400					12	12,5	93	1100
178.400	1	414	400					13	12,5	93	1100
179.400	4	414	400					5	12,5	93	1000
180.400	4	414	400					13	12,5	93	1000
188.400	1	413	400					9	12,5	93	1000
518.400	5	416	400	0				13	12,5	93	1000
519.400	5	416	400	0				13	12,5	93	1000
520.400	5	416	400	0				11	12,5	93	1100
521.400	6	416	400	0				11	12,5	93	1100
191.500	2	422	500					16	12,5	93	1000
193.500	3	422	500					16	12,5	93	1000
194.500	3	422	500					18	12,5	93	1000
195.500	3	422	500					18	12,5	93	1000
198.500	3	422	500					16	12,5	93	1000
199.500	3	422	500					21	12,5	93	1000
200.500	3	422	500					21	12,5	93	1000
201.500	3	422	500					21	12,5	93	1000

Table 2. Length, span and mass of slab, length of bearing (t_b), shear span (a) and distance between two line loads (a_1), average depth of section (H_{ave}), average web width ($b_w =$ sum of individual web widths $b_{w,i}$), average depth of hollow core (H_o), average thickness of concrete below hollow core (t_{low}), average distance from lower strands to the soffit ($d_{p,low}$) and from upper strand to the top fibre ($d_{p,up}$).

Test	Length mm	Span mm	Mass kg	t_b mm	$a/(a_1)$ mm	H_{ave} mm	b_{ave} mm	b_w mm	H_o mm	t_{low} mm	$d_{p,low}$ mm	$d_{p,up}$ mm
31.200	6643	6603	2000	40	917	200	1162	239	153	19	39	
33.200	4998	4958	1490	40	689	202	1163	238	157	19	40	
40.200	6257	6217	2290	40	863	202	1158	293	138	34	39	
63.200	4006	3966	1250	40	551	202	1158	262	144	20	38	
74.265	5199	5159	2230	40	717	257	1156	219	184	43	40	
98.265	5253	5213	2240	40	724	260	1157	228	175	42	36	
104.265	5004	4964	2280	40	689	268	1158	244	172	41	45	
107.265	5007	4967	2210	40	690	255	1158	239	171	41	39	
109.265	4997	4957	2160	40	688	262	1157	242	174	34	39	
110.265	5015	4975	2160	40	691	261	1158	220	177	43	32	
113.265	4997	4957	2220	40	688	267	1155	226	176	41	34	
114.265	5285	5245	2280	40	728	265	1159	232	171	36	34	40
115.265	4963	4923	2000	40	684	258	1156	215	183	31	40	
116.265	4507	4457	1920	50	663	270	1160	222			45	
501.265	5501	4000	2310	75	968	259	1153	224	186	38	41	
502.265	5501	4000	2310	75	968	259	1153	224	186	38	41	
503.265	6000	5940	2560	60	970	260	1161	221	180	38	34	
504.265	6000	4940	2560	60	970	260	1161	221	180	38	34	
505.265	5998	5938	2500	60	970	260	1157	216	183	39	35	
506.265	5998	5000	2500	60	970	260	1157	216	183	39	35	
507.265	5995	5935	2520	60	970	263	1156	218	182	36	37	
508.265	5995	5000	2520	60	970	263	1156	218	182	36	37	
509.265	5996	5936	2450	60	970	184	1155	217	184	34	36	
510.265	5996	5000	2450	60	970	184	1155	217	184	34	36	
511.265	5999	5940	2610	60	1170	263	1150	221	176	40	40	
512.265	6001	5940	2680	60	1170	262	1150	223	174	40	39	
132.320	7002	6942	4200	60	810/300	311	1165	254	161	64	42	
133.320	6995	6935	4310	60	810/300	322	1160	261	164	70	48	
134.320	6990	6930	4330	60	970/300	327	1161	243	174	68	47	
136.320	5009	4959	2410	50	800	321		313			42	
138.320	6990	6940	3410	50	800	321		299			41	
139.320	7001	6951	3470	50	800	320		304			40	
146.320	5890	5850	3060	40	813	303	1154	256	211	44	33	
148.320	5985	5945	3100	40	826	310	1149	263	213	40	51	49
151.320	6003	5963	3060	40	828	311	1163	270	211	46	48	
513.320	9594	9527	4360	70	1265	319	1162	258	243	36	51	22
514.320	7198	7118	3810	80	1160	315	1165	309	222	38	43	
515.320	7200	7120	3800	80	1160	314	1165	311	222	38	42	
516.320	7995	5800	3880	80	760	321	1153	289	216	36	38	
517.320	7991	5800	3830	80	760	321	1153	287	216	37	39	

Table 2. Continued.

Test	Length mm	Span mm	Mass kg	t_b mm	$a/(a_1)$ mm	H_{ave} mm	b_{ave} mm	b_w mm	H_o mm	t_{low} mm	$d_{p,low}$ mm	$d_{p,up}$ mm
159.370	6994	6934	4060	60	960/300	358	1144	270	236	56	39	
160.370	7002	6942	4060	60	960/300	359	1145	272	237	54	40	
161.370	6993	6933	4070	60	1145/300	357	1145	276	234	57	39	
162.400	10017	9937	5480	80	1380	397	1172	284	306	41	53	
178.400	7626	7546	4510	80	1048	402	1158	286	299	49	38	
179.400	6496	6406	3670	90	1000	402		262			35	
180.400	6988	6898	4100	90	1000	405		278			46	
188.400	8000	7920	4430	80	1100	407	1161	285	312	48	39	
518.400	8390	8290	4580	100	1150	390	1152	293	310	38	41	
519.400	8390	7150	4580	100	1150	390	1152	293	310	38	41	
520.400	5504	4000	3010	75	968	396	1152	291	307	41	36	
521.400	5504	4000	3010	75	968	396	1152	291	307	41	36	
191.500	10995	10915	7640	80	1364	498	1169	325	400	40	53	
193.500	8470	8390	5960	80	1350/300	500	1163	335	399	43	56	
194.500	8499	8419	5820	80	1350/300	501	1169	312	405	36	58	
195.500	8495	8415	5920	80	1350/300	496	1163	331	396	39	49	
198.500	8492	8412	6000	80	1475/300	503	1167	324	398	40	47	
199.500	8516	8436	6080	80	1350/300	497	1177	326	392	42	52	
200.500	8510	8430	6120	80	1475/300	494	1171	327	396	43	53	
201.500	8512	8432	6040	80	1600/300	495	1174	322	398	42	51	

Table 3. Two largest slippages in upper strands ($S_{1,up}$, $S_{2,up}$), four largest slippages in lower strands (S_1 , S_2 , S_3 , S_4), measured mean core strength ($f_{C50,mean}$) and standard deviation of the measured core strength (δ_{C50}).

Slab	$S_{1,up}$ mm	$S_{2,up}$ mm	S_1 mm	S_2 mm	S_3 mm	S_4 mm	$f_{C50,mean}$ MPa	δ_{C50} MPa
31.200			0,4	0,4	0,3	0,3	54,8	3,8
33.200			0,4	0,3	0,2	0,2	52,8	3,2
40.200			1,0	0,8	0,5	0,4	76,5	3,8
63.200			0,6	0,4	0,4	0,4	56,6	2,5
74.265			1,0	0,6	0,6	0,6	77,9	3,2
98.265			1,1	1,0	1,0	0,9	71,3	4,2
104.265			1,0	0,5	0,5	0,4	47,6	4,0
107.265			1,0	1,0	0,6	0,3	47,9	3,1
109.265			2,2	1,3	1,1	1,0	56,7	3,0
110.265			0,7	0,7	0,6	0,6	56,5	2,6
113.265			0,8	0,5	0,5	0,4	61,9	2,5
114.265	0,2	0,1	0,6	0,5	0,4	0,4	60,2	2,7
115.265			0,9	0,8	0,6	0,5	63,2	4,9
116.265			0,7	0,6	0,5	0,5	58,3 ¹⁾	-
501.265			1	0,8	0,7	0,6	67,1	2,4
502.265			1	0,8	0,7	0,6	67,1	2,4
503.265			1,2	1,1	1,1	1,1	72	4,9
504.265			1,2	1,1	1,1	1,1	72	4,9
505.265			1,7	1,5	1,4	1,2	70,8	4,3
506.265			1,7	1,5	1,4	1,2	70,8	4,3
507.265			2,3	1,7	1,4	1,2	68 ²⁾	8,1
508.265			2,3	1,7	1,4	1,2	68 ²⁾	8,1 ¹⁾
509.265			1,3	1,3	1	1	65,8	2,1
510.265			1,3	1,3	1	1	65,8	2,1
511.265			1,3	0,9	0,8	0,7	67,8	2,5
512.265			1,2	0,7	0,6	0,6	67,8	2,9
132.320			0,9	0,7	0,6	0,5		
133.320			1,5	1,3	1,3	1,3	68,0	1,9
134.320			1,3	1,2	1,1	1,0	68,0	1,9
136.320			0,8	0,5	0,4	0,3		
138.320			1,2	1,1	1,0	0,9		
139.320			1,1	0,7	0,7	0,6		
146.320			0,4	0,4	0,4	0,3	57,0	3,6
148.320	0,2	0,1	0,6	0,4	0,3	0,3	46,8	2,0
151.320			0,6	0,5	0,5	0,4	66,8	5,5
513.320			1,9	1,9	1,8	1,8	62,1	4,6
514.320			2,5	1,7	1,4	1,3	61,8	2,4
515.320			1,7	1,5	1,3	1,2	61,8	2,4
516.320			1	0,9	0,8	0,7	64,3	2,6
517.320			0,8	0,8	0,8	0,7	64,8	1,2

¹⁾ Strength measured from three cores: 58, 58 and 59 MPa

²⁾ Strength measured from six cores, 1 result only 54 MPa, considerably lower than the others

Table 3. Continued.

Slab	$S_{1,up}$ mm	$S_{2,up}$ mm	S_1 mm	S_2 mm	S_3 mm	S_4 mm	$f_{C50,mean}$ MPa	δ_{C50} MPa
159.370			1,4	1,1	0,8	0,7		
160.370			0,6	0,5	0,5	0,5	72,2	2,1
161.370			0,5	0,5	0,5	0,5	72,2	2,1
162.400			1,4	1,0	0,8	0,8	65,2	5,0
178.400			1,3	1	0,9	0,8	71,5	4,0
179.400			1,5	0,9	0,6	0,6		
180.400			2,3	1,7	1,7	1,5		
188.400			1,0	0,8	0,5	0,5	55,5	2,9
518.400			1,9	1,1	0,9	0,9	67,3	1,7
519.400			1,9	1,1	0,9	0,9	67,3	1,7
520.400			1,6	1,6	1,5	1,5	64,2	2,5
521.400			1,6	1,6	1,5	1,5	64,2	2,5
191.500			0,9	0,9	0,7	0,7	70,8	1,1
193.500			0,9	0,9	0,8	0,8	70,8	1,1
194.500			1,5	1,2	1,0	0,7	67,3 ¹⁾	-
195.500			2,0	1,2	1,2	1,0		
198.500			0,8	0,7	0,7	0,6	76,4	2,6
199.500			2,1	1,5	1,4	0,8	74,7	5,3
200.500			1,7	1,4	1,1	1,0	74,7	5,3
201.500			2,0	1,8	1,2	1,0	74,7	5,3

¹⁾ Strength measured from three cores: 70, 64 and 68 MPa

Table 4. Date of casting and loading, age at loading, load when first crack width (flexural) exceeds 0,2 mm (P_{cr}), load at failure (P_{fail}), shear force at loaded support due to self weight (V_g) and distance of crack from support on the top surface (c_1) and at the bottom surface (c_2). Both c_1 and c_2 are mean of two values measured on opposite edges of the slab.

Test	Date of casting	Date of loading	Age at loading [d]	P_{cr} kN	P_{fail} kN	V_g kN	c_1/c_2	Note
31.200	31.1.01	21.3.01	49	57,4	80,4	9,8	300/100	
33.200	31.1.01	2.4.01	61	80,4	108,3	7,3	450/150	
40.200	28.10.92	26.11.92	29	82,8	94,8	11,2		
63.200	16.11.01	14.2.02	90	122,4	131,4	6,1		
74.265	25.1.95	25.1.95	0	116,4	148,9	10,9	700/440	
98.265	3.12.99	19.1.00	47	194,4	208,5	10,9	700/0	
104.265	8.7.98	22.9.98	76	85,8	124,9	11,1		
107.265	10.12.99	17.1.00	38	89,5	123,4	10,8		
109.265	10.12.01	6.2.02	58	-	177,7	10,5		
110.265	3.8.94	27.1.95	177	163,4	184,4	10,5		
113.265	4.9.97	28.1.98	146	107,2	170,4	10,8		
114.265	17.7.98	7.10.98	82	163,1	179,4	11,1		
115.265	1.7.99	5.1.00	188	113,4	166,4	9,7		
116.265	-	31.7.02			226,5	9,3		
501.265	17.10.91	13.11.91	27		272,1	7,1	900/180	Strength measured 29.11.
502.265	17.10.91	13.11.91	27		261,1	7,1	900/120	Strength measured 29.11.
503.265	15.9.93	11.10.93	26		233,7	12,4	850/170	
504.265	15.9.93	11.10.93	26		209,0	9,9	450/100	
505.265	11.11.93	21.12.93	40		240,4	12,2	810/220	Strength measured 23.12.
506.265	11.11.93	21.12.93	40		256,4	9,8	540/70	Strength measured 23.12.
507.265	8.11.03	21.12.93	43		219,4	12,2	360/0	Strength measured 23.12.
508.265	8.11.03	21.12.93	43		219,4	9,9	390/0	Strength measured 23.12.
509.265	21.1.94	11.3.94	49		211,0	11,9	600/30	
510.265	21.1.94	11.3.94	49		237,1	9,6	650/100	
511.265	10.10.94	17.11.94	38		264,9	12,7	1100/30	
512.265	10.10.94	17.11.94	38		266,5	13,0	1100/30	
132.320	12.2.02	22.4.02	69	-	255,4	20,4	750/200	
133.320	28.1.02	23.4.02	85	-	275,4	21,0	550/150	
134.320	28.1.02	23.4.02	85	-	269,4	21,1	550/200	
136.320	20.11.00	18.12.00	28	-	189,5	11,7	700/300	
138.320	31.7.02	30.8.02	30	-	298,0	16,6	600/160	
139.320	8.10.02	8.11.02	31	-	252,0	16,9	630/270	
146.320	21.11.94	31.1.95	71	133,4	198,8	14,9		
148.320	3.12.96	23.1.97	51	223,4	238,8	15,1		
151.320	24.5.99	5.1.00	226	153,4	240,4	14,9		
513.320	21.11.01	24.1.02	64		230,7	21,3	450/0	
514.320	14.1.98	1.4.98	77		332,8	18,5	650/50	
515.320	14.1.98	1.4.98	77		328,8	18,4	800/100	
516.320	7.3.03	12.5.03	66		253,9	11,8 ¹⁾	800/200	Strength measured 17.4
517.320	7.3.03	13.5.03	67		219,8	11,7 ¹⁾	800/50	Strength measured 8.5

1) The weight of cast-in-itu concrete at passive end is taken into account.

Table 4. Continued.

Test	Date of casting	Date of loading	Age at loading [d]	P_{cr} kN	P_{fail} kN	V_g kN	c_1/c_2	Note
159.370	21.10.02	18.11.02	28	-	252,7	19,8	500/100	
160.370	9.10.02	6.11.02	28	-	286,4	19,8	700/250	
161.370	9.10.02	6.11.02	28	-	262,4	19,8	750/300	
162.400	28.4.93	17.8.93	111	186,4	287,4	26,7		1
178.400	28.10.99	20.1.00	84	-	269,4	21,9	1000/0	
179.400	10.11.00	15.12.00	35	-	262,5	17,8	650/250	
180.400	21.10.02	18.10.02	-3	-	305,0	19,9	760/180	
188.400	28.11.97	29.1.98	62	187,4	271,4	21,5		
518.400	29.10.99	8.12.99	40		432,7	22,2	900/350	
519.400	29.10.99	8.12.99	40		507,0	18,6	750/180	Strength measured 10.12.
520.400	17.10.91	14.11.91	28		443,2	9,2	800/100	Strength measured 29.11.
521.400	17.10.91	14.11.91	28		382,0	9,2	800/100	Strength measured 29.11.
191.500	28.3.00	5.5.00	38	208,4	326,0	37,2	900/150	
193.500	28.3.00	3.5.00	36	-	386,0	29,0	1000/150	
194.500	3.4.00	4.5.00	31	-	452,0	28,3	1000/350	
195.500	29.5.00	8.6.00	10	-	332,0	28,8	1350/150	
198.500	8.1.01	22.3.01	73	-	442,0	29,2	750/250	
199.500	4.6.02	31.7.02	57	-	528,0	29,6	900/250	
200.500	4.6.02	2.8.02	59	-	485,0	29,8	1200/300	
201.500	4.6.02	5.8.02	62	-	462,0	29,4	1200/400	

Table 5. Observed shear resistance V_{obs} and shear resistance calculated using EC2 method (V_{pre}). Two different losses of prestress (5% and 15%) and two values of tensile strength have been assumed.

		Mean tensile strength				Characteristic tensile strength			
Loss of prestress		5%		15%		5%		15%	
Slab	V_{obs} kN	V_{pre} kN	$\frac{V_{obs}}{V_{pre}}$	V_{pre} kN	$\frac{V_{obs}}{V_{pre}}$	V_{pre} kN	$\frac{V_{obs}}{V_{pre}}$	V_{pre} kN	$\frac{V_{obs}}{V_{pre}}$
31.200	90.2	145.7	0.619	143.9	0.626	107.3	0.840	105.5	0.854
33.200	115.6	142.7	0.810	141.0	0.819	105.2	1.099	103.4	1.118
40.200	106.0	218.7	0.484	216.0	0.491	161.1	0.658	158.4	0.669
63.200	137.5	165.7	0.830	163.8	0.839	121.6	1.131	119.7	1.148
98.265	219.4	223.8	0.980	220.5	0.995	166.1	1.321	162.9	1.347
104.265	136.0	163.5	0.832	162.4	0.837	117.9	1.154	116.8	1.165
107.265	134.2	165.2	0.812	164.1	0.818	119.3	1.125	118.1	1.136
109.265	188.2	207.6	0.907	204.6	0.920	153.9	1.223	151.0	1.247
110.265	194.9	186.9	1.043	184.7	1.055	137.7	1.416	135.4	1.439
113.265	181.2	195.8	0.926	194.2	0.933	141.9	1.277	140.3	1.291
114.265	190.5	209.0	0.912	206.1	0.924	154.6	1.232	151.8	1.255
115.265	176.1	183.7	0.959	181.9	0.968	134.0	1.315	132.2	1.332
501.265	213.4	224.9	0.949	221.2	0.965	168.5	1.266	164.8	1.295
502.265	205.0	224.9	0.912	221.2	0.927	168.5	1.217	164.8	1.244
503.265	208.0	221.0	0.941	217.5	0.956	165.0	1.261	161.5	1.288
504.265	177.8	221.0	0.805	217.5	0.818	165.0	1.078	161.5	1.101
505.265	213.3	214.6	0.994	211.2	1.010	160.0	1.333	156.7	1.361
506.265	216.5	214.6	1.009	211.2	1.025	160.0	1.353	156.7	1.381
507.265	195.8	197.3	0.992	194.3	1.008	147.1	1.331	144.1	1.359
508.265	186.7	197.3	0.946	194.3	0.961	147.1	1.269	144.1	1.296
509.265	188.4	213.3	0.883	210.0	0.897	159.0	1.185	155.8	1.210
510.265	200.7	213.3	0.941	210.0	0.956	159.0	1.262	155.8	1.289
511.265	225.4	219.9	1.025	216.4	1.042	164.1	1.374	160.7	1.403
512.265	227.0	221.5	1.025	218.0	1.042	165.3	1.373	161.9	1.403
133.320	296.4	306.3	0.968	301.6	0.983	228.2	1.299	223.6	1.325
134.320	290.5	285.2	1.019	280.9	1.034	212.5	1.367	208.2	1.395
146.320	213.7	247.3	0.864	245.1	0.872	180.0	1.188	177.8	1.202
148.320	253.9	246.6	1.030	242.7	1.046	183.7	1.382	180.0	1.411
151.320	255.3	292.9	0.872	289.3	0.882	215.6	1.185	212.0	1.205
513.320	221.3	309.8	0.714	303.4	0.730	235.0	0.942	229.0	0.967
514.320	297.1	378.7	0.784	371.2	0.800	286.2	1.038	279.2	1.064
515.320	293.7	381.1	0.771	373.6	0.786	288.0	1.020	281.0	1.045
516.320	232.5	359.7	0.646	353.0	0.659	270.8	0.858	264.4	0.879
517.320	202.7	364.9	0.556	358.0	0.566	274.7	0.738	268.3	0.756

Table 5. Continued

		Mean tensile strength				Characteristic tensile strength			
Loss of prestress		5%		15%		5%		15%	
Slab	V_{obs} kN	V_{pre} kN	$\frac{V_{obs}}{V_{pre}}$	V_{pre} kN	$\frac{V_{obs}}{V_{pre}}$	V_{pre} kN	$\frac{V_{obs}}{V_{pre}}$	V_{pre} kN	$\frac{V_{obs}}{V_{pre}}$
160.370	306.2	396.2	0.773	389.4	0.786	296.9	1.031	290.4	1.054
161.370	282.2	402.1	0.702	395.2	0.714	301.3	0.937	294.7	0.958
162.400	314.1	432.1	0.727	423.8	0.741	325.8	0.964	318.0	0.988
178.400	291.3	475.4	0.613	465.7	0.626	360.1	0.809	351.0	0.830
188.400	292.9	381.7	0.768	375.7	0.780	284.5	1.030	278.7	1.051
518.400	394.9	500.9	0.788	490.0	0.806	381.6	1.035	371.2	1.064
519.400	444.0	500.9	0.886	490.0	0.906	381.6	1.164	371.2	1.196
520.400	345.2	458.8	0.753	450.0	0.767	345.5	0.999	337.4	1.023
521.400	391.2	458.8	0.853	450.0	0.869	345.5	1.132	337.4	1.159
191.500	363.2	694.4	0.523	679.4	0.535	528.6	0.687	514.2	0.706
193.500	415.0	718.3	0.578	702.6	0.591	547.1	0.759	532.1	0.780
198.500	471.2	702.5	0.671	687.5	0.685	534.5	0.882	520.1	0.906
199.500	557.6	717.7	0.777	700.1	0.796	551.3	1.011	534.9	1.042
200.500	514.8	721.8	0.713	704.0	0.731	554.7	0.928	538.1	0.957
201.500	491.4	709.5	0.693	692.1	0.710	545.1	0.902	528.8	0.929

Table 6. Observed shear resistance V_{obs} and shear resistance calculated using Yang's method (V_{pre}). Two different losses of prestress (5% and 15%) and two values of tensile strength have been assumed.

Loss of prestress	Mean tensile strength					Characteristic tensile strength			
	5%			15%		5%		15%	
	Slab	V_{obs} kN	V_{pre} kN	$\frac{V_{obs}}{V_{pre}}$	V_{pre} kN	$\frac{V_{obs}}{V_{pre}}$	V_{pre} kN	$\frac{V_{obs}}{V_{pre}}$	V_{pre} kN
31.200	90.2	128.040	0.704	126.690	0.712	93.1	0.969	92.0	0.980
33.200	115.6	124.560	0.928	123.340	0.937	90.2	1.281	89.3	1.294
40.200	106.0	193.440	0.548	190.550	0.556	142.9	0.742	140.4	0.755
63.200	137.5	148.070	0.928	146.080	0.941	108.9	1.263	107.2	1.283
98.265	219.4	223.660	0.981	218.810	1.003	169.8	1.292	165.4	1.327
104.265	136.0	149.470	0.910	148.080	0.918	108.7	1.251	107.4	1.266
107.265	134.2	154.460	0.869	152.710	0.879	113.2	1.185	111.6	1.202
109.265	188.2	202.300	0.930	198.280	0.949	152.6	1.234	148.9	1.264
110.265	194.9	185.820	1.049	182.170	1.070	139.9	1.393	136.7	1.426
113.265	181.2	181.470	0.999	179.530	1.009	132.6	1.367	130.8	1.386
114.265	190.5	205.210	0.928	201.120	0.947	154.7	1.231	151.0	1.261
115.265	176.1	172.850	1.019	170.650	1.032	127.1	1.386	125.1	1.408
501.265	213.4	217.170	0.983	212.560	1.004	164.5	1.297	160.4	1.330
502.265	205.0	217.170	0.944	212.560	0.965	164.5	1.247	160.4	1.278
503.265	208.0	224.940	0.925	219.450	0.948	172.5	1.206	167.5	1.242
504.265	177.8	224.940	0.791	219.450	0.810	172.5	1.031	167.5	1.062
505.265	213.3	216.830	0.984	211.740	1.007	165.7	1.287	161.1	1.324
506.265	216.5	216.830	0.998	211.740	1.022	165.7	1.306	161.1	1.344
507.265	195.8	196.010	0.999	191.690	1.021	149.0	1.314	145.1	1.349
508.265	186.7	196.010	0.953	191.690	0.974	149.0	1.253	145.1	1.287
509.265	188.4	213.920	0.881	209.040	0.901	163.1	1.155	158.7	1.188
510.265	200.7	213.920	0.938	209.040	0.960	163.1	1.231	158.7	1.265
511.265	225.4	213.500	1.056	209.110	1.078	161.3	1.397	157.4	1.432
512.265	227.0	216.740	1.047	212.120	1.070	164.3	1.382	160.1	1.418
133.320	296.4	304.610	0.973	298.270	0.994	230.9	1.284	225.0	1.317
134.320	290.5	286.280	1.015	280.190	1.037	217.2	1.337	211.6	1.373
146.320	213.7	245.990	0.869	240.850	0.887	186.9	1.143	182.0	1.174
148.320	253.9	239.700	1.059	234.120	1.085	183.0	1.388	177.9	1.427
151.320	255.3	282.920	0.902	276.940	0.922	214.2	1.192	208.8	1.223
513.320	221.3	243.210	0.910	241.980	0.915	173.6	1.275	172.6	1.282
514.320	297.1	322.890	0.920	318.580	0.932	238.0	1.248	233.8	1.271
515.320	293.7	325.060	0.903	320.700	0.916	239.6	1.226	235.4	1.248
516.320	232.5	317.230	0.733	312.410	0.744	234.9	0.990	230.2	1.010
517.320	202.7	320.080	0.633	315.370	0.643	236.7	0.856	232.1	0.873

Table 6. Continued.

		Mean tensile strength				Characteristic tensile strength			
Loss of prestress		5%		15%		5%		15%	
Slab	V_{obs} kN	V_{pre} kN	$\frac{V_{obs}}{V_{pre}}$	V_{pre} kN	$\frac{V_{obs}}{V_{pre}}$	V_{pre} kN	$\frac{V_{obs}}{V_{pre}}$	V_{pre} kN	$\frac{V_{obs}}{V_{pre}}$
160.370	306.2	373.790	0.819	367.270	0.834	280.9	1.090	274.4	1.116
161.370	282.2	380.950	0.741	374.140	0.754	286.7	0.984	279.9	1.008
162.400	314.1	338.710	0.927	337.670	0.930	241.2	1.302	240.0	1.309
178.400	291.3	443.970	0.656	434.480	0.670	331.5	0.879	324.2	0.899
188.400	292.9	360.550	0.812	354.270	0.827	266.9	1.098	261.2	1.122
518.400	394.9	405.680	0.973	401.820	0.983	292.0	1.352	289.8	1.363
519.400	444.0	405.680	1.095	401.820	1.105	292.0	1.521	289.8	1.532
520.400	345.2	384.550	0.898	381.030	0.906	277.3	1.245	274.9	1.256
521.400	391.2	384.550	1.017	381.030	1.027	277.3	1.411	274.9	1.423
191.500	363.2	541.330	0.671	539.860	0.673	379.0	0.958	379.9	0.956
193.500	415.0	548.300	0.757	547.820	0.758	380.9	1.089	382.9	1.084
198.500	471.2	565.680	0.833	562.330	0.838	401.3	1.174	400.3	1.177
199.500	557.6	538.640	1.035	538.090	1.036	373.3	1.494	375.7	1.484
200.500	514.8	536.110	0.960	536.190	0.960	370.1	1.391	373.1	1.380
201.500	491.4	535.640	0.917	534.780	0.919	372.1	1.321	374.2	1.313

Author(s) Pajari, Matti			
Title Resistance of prestressed hollow core slabs against web shear failure			
Abstract Eurocode 2 presents a design method for the shear resistance, which according to harmonized standard EN 1168 is to be used for the web shear failure of prestressed hollow core slabs. To check the validity of the method, 49 shear tests on hollow core slabs with thickness 200–500 mm have been analysed. The Eurocode 2 method overestimated the mean shear resistance of all tested slab types. For 200 mm slabs and slabs with flat webs the overestimation was tens of percent. When the characteristic values of experimental and theoretical resistance were compared, the fit was better but there was still a considerable overestimation for 200 mm slabs and for the slabs with flat webs. On the other hand, the Eurocode 2 method was (over)conservative for 265 mm and 320 mm slabs with circular voids. The Eurocode 2 method ignores the shear stresses due to the transfer of the prestressing force. When these stresses were taken into account applying Yang's method, the accuracy for 265 mm and 320 mm slabs with circular voids was the same as when using the Eurocode 2 method but much better for the other slabs. Based on the results of the comparison, Yang's method for design against web shear failure should replace the present method in Eurocode 2. It is not acceptable, however, to adopt a design method which overestimates the characteristic resistance of some product type by 10% as Yang's method seems to do. Whether this is really the case, is still an open question because the number of tests on the problematic slabs was small. Furthermore, due to the nature of the type approval tests, some test specimens may have been weaker than the slabs typical of normal production. The Eurocode 2 method should not be used for slabs with flat webs without a reduction factor, and its applicability to other slab types should always be verified either numerically or experimentally before it is used.			
Keywords hollow core slab, prestress, shear, test, resistance, concrete, precast, structure, design, Eurocode			
Activity unit VTT Building and Transport, Kemistintie 3, P.O.Box 1805, FI-02044 VTT, Finland			
ISBN 951-38-6709-9 (soft back ed.) 951-38-6552-5 (URL: http://www.vtt.fi/inf/pdf/)			Project number R4SU00547
Date April 2005	Language English	Pages 47 p. + app. 15 p.	Price B
Name of project Shear resistance of prestressed hollow core slabs		Commissioned by Confederation of Finnish Construction Industries RT, VTT Technical Research Centre of Finland	
Series title and ISSN VTT Tiedotteita – Research Notes 1235-0605 (soft back edition) 1455-0865 (URL: http://www.vtt.fi/inf/pdf/)		Sold by VTT Information Service P.O.Box 2000, FI-02044 VTT, Finland Phone internat. +358 20 722 4404 Fax +358 20 722 4374	

In the future, the European prestressed hollow core slabs will be designed in accordance with the European standards EN 1168 and Eurocode 2. To check the validity of the future design method for the shear resistance, 49 shear tests on hollow core slabs with thickness 200–500 mm have been analysed.

When compared with the test results, the shear resistance predicted by the Eurocode 2 method was conservative for some slab types and nonconservative for some others. Another design method proposed by Yang gave a much better fit with test results. For this reason it is proposed that the present design method in Eurocode 2 will be replaced by Yang's method, possibly modified with a calibration factor.

Tätä julkaisua myy
VTT TIETOPALVELU
PL 2000
02044 VTT
Puh. 020 722 4404
Faksi 020 722 4374

Denna publikation säljs av
VTT INFORMATIONSTJÄNST
PB 2000
02044 VTT
Tel. 020 722 4404
Fax 020 722 4374

This publication is available from
VTT INFORMATION SERVICE
P.O.Box 2000
FI-02044 VTT, Finland
Phone internat. + 358 20 722 4404
Fax + 358 20 722 4374
